Monitoring ecosystem stress and carbon uptake with reflectance and fluorescence measurements

Elizabeth M. Middleton

Fred Huemmrich
Petya Campbell
Qingyuan Zhang
Joanna Joiner
HyspIRI team members
NASA Goddard Space Flight Center

HyspIRI Science Workshop 2017
Pasadena, California
October 17-19, 2017

TOPICS

I. Prototype HyspIRI Products using
EO-1 Hyperion and other Spectrometers

II. A Study using fAPARchl and
Far-Red Solar Induced Fluorescence

Product Prototypes

- Characterization of canopy biophysical parameters and function
  - Using integrated leaf- canopy models with the spectra to derive canopy bio-physical and bio-chemistry parameters
  - Using machine learning and empirical models to map productivity
- Spectral time series
  - Calibration sites / deserts: consistency/stability of derived reflectance
  - Vegetation: characterizing the dynamics in canopy function, field data are key (e. g. flux sites, instrumented, *in situ* field collections)
- Spectral Continuity of Current Multispectral Bands, VIs and Products

The EO-1 Image Archive

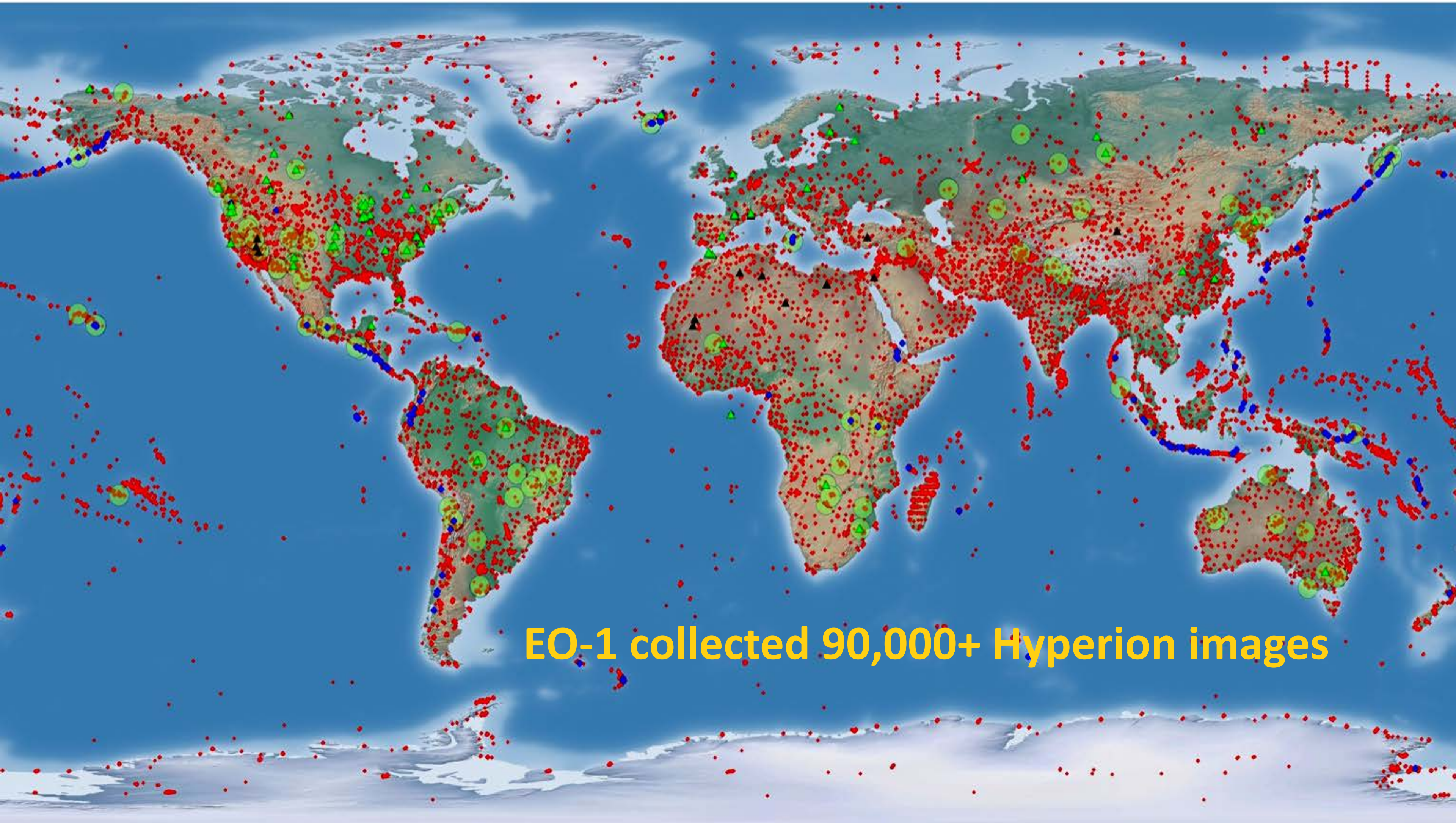

EO-1 Observations • MSO Sites ▲ CEOS Sites ▲ Volcanoes ◆ > 10 Observations ○

The EO-1 Image Collections

Collection	Scenes total (<10% clouds)	Primary sensor	Field Earth Observation Networks / Efforts
1 ABoVE	1367(293)	ALI	Arctic-Boreal Vulnerability Experiment, NASA/TE
2 CEOS/WGCV	1022(568)	Hyperion	The CEOS Working Group on Calibration & Validation
3 **FLUXNET**	9680(3552)	Hyperion	Network of eddy covariance flux measurements of carbon, water vapor and energy exchange
4 LTER	1181(412)	ALI	The Long Term Ecological Research Network
5 NEON	973(314)	Hyperion	The National Ecological Observatory Network
6 SIGEO	1125(298)	Hyperion	The Smithsonian Institution Global Earth Observatory, ForestGEO
7 SpecNet	1245(305)	Hyperion	SpecNet - Linking optical measurements with flux sampling
8 Volcanoes	19155(3070)	Hyperion	Vocano Sensorweb, NASA/JPL
9 UNESCO-WCH Reserves	992(172)	ALI/Hyperion	UNESCO World Cultural Heritage, Nature Reserves

CEOS/WGCV

Volcano Sensorweb

Smithsonian Tropical Research Institute

HyspIRI Studies of Ecosystem Processes and Characteristics: near Barrow, AK

Addressing questions of terrestrial ecosystem diversity, biochemistry,and function

Biodiversity

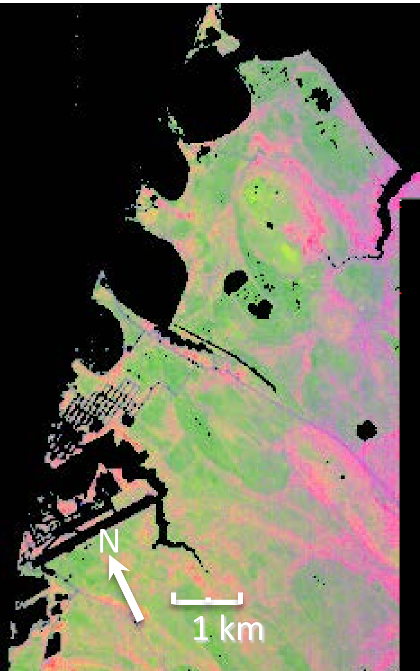

Tundra plant cover type fractions
R-Vascular Plants
G-Moss
B-Lichen

Biochemistry

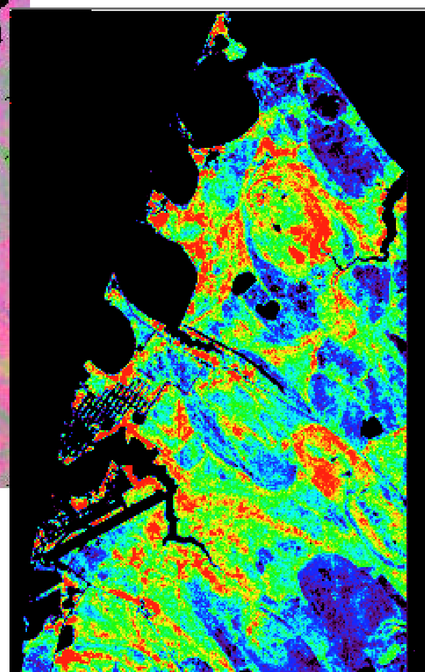

Chlorophyll Index

Ecosystem Function

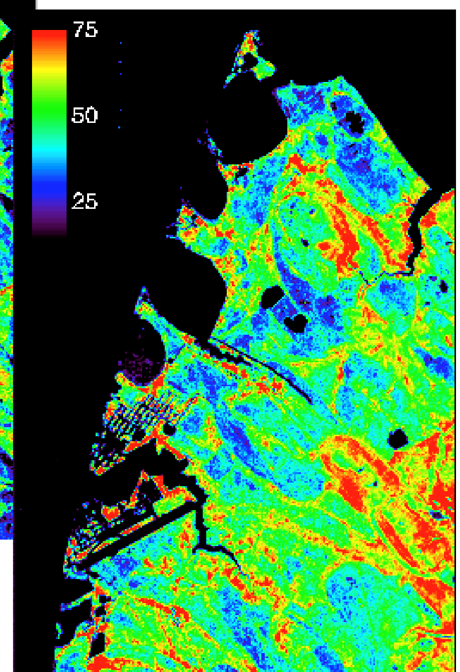

Photosynthetic light use efficiency (mol C mol^{-1} absorbed quanta X 1000)

Hyperion image of tundra near Barrow, AK, USA, July 20, 2009
Huemmrich et al. JSTARS 2013

- Plant type distribution affects ecosystem processes and response to climate change
- Biochemistry is diagnostic of responses to environmental conditions, e.g. soil nutrients, water availability
- Ecosystem function shows the spatial patterns in productivity over an area considered a single vegetation type in models

HyspIRI Studies of Ecosystem Processes and Characteristics: LUE

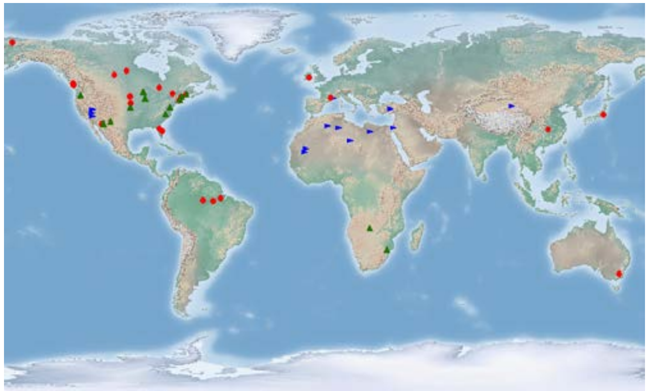

Utilize EO-1 Hyperion's capacity to observe globally-distributed sites over a wide range of vegetation types

Matched flux data from LaThuile Fluxnet Synthesis with Hyperion imagery for 33 globally distributed flux tower sites

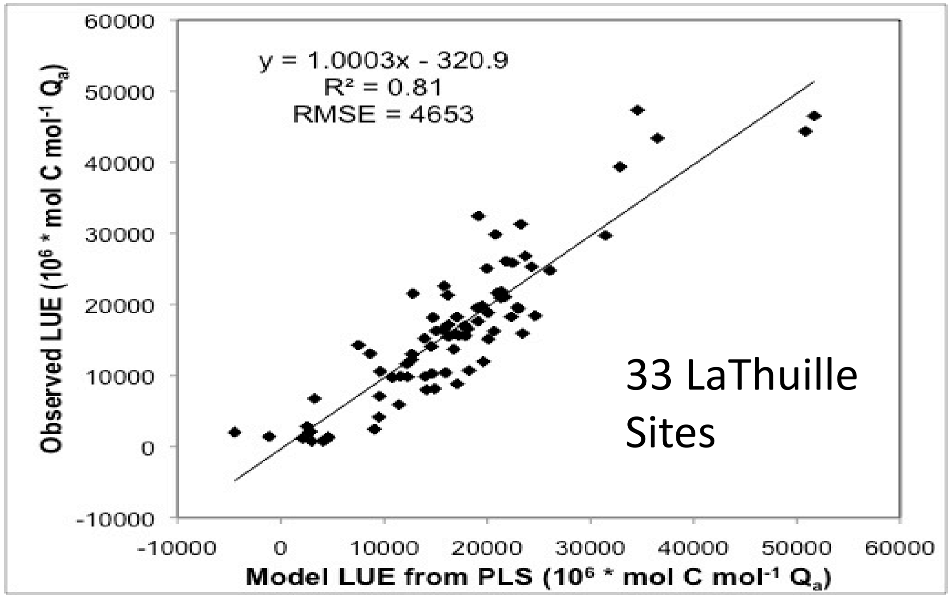

Light Use Efficiency (LUE) estimated from reflectance using PLS regression of spectra to observed LUE from flux towers

Florida Slashpine

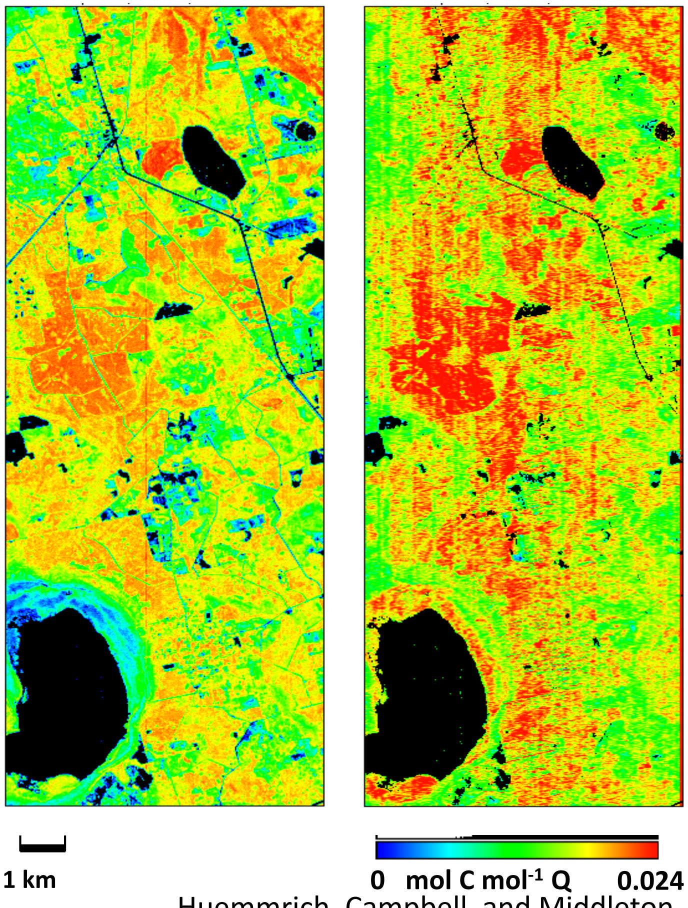

Huemmrich, Campbell, and Middleton

HyspIRI Studies of Ecosystem Processes and Characteristics: NEP

Using EO-1 / Hyperion for seasonal dynamics and ecosystem function relies on spectral stability and repeated coverage

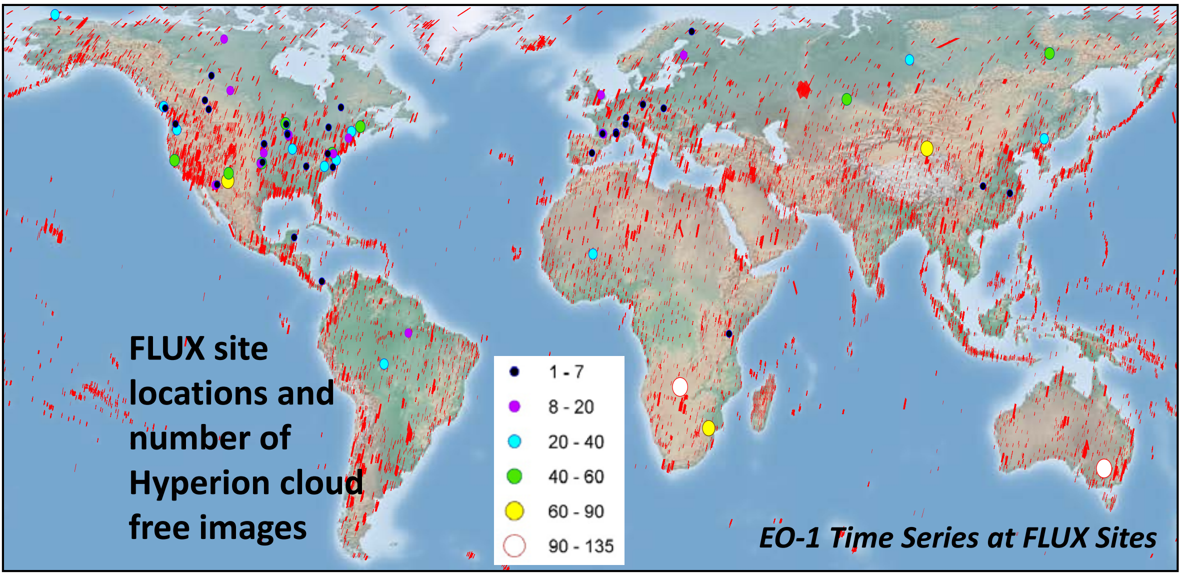

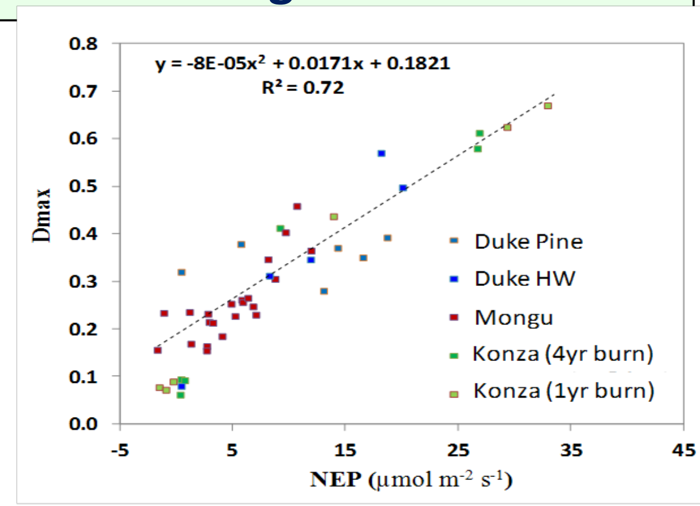

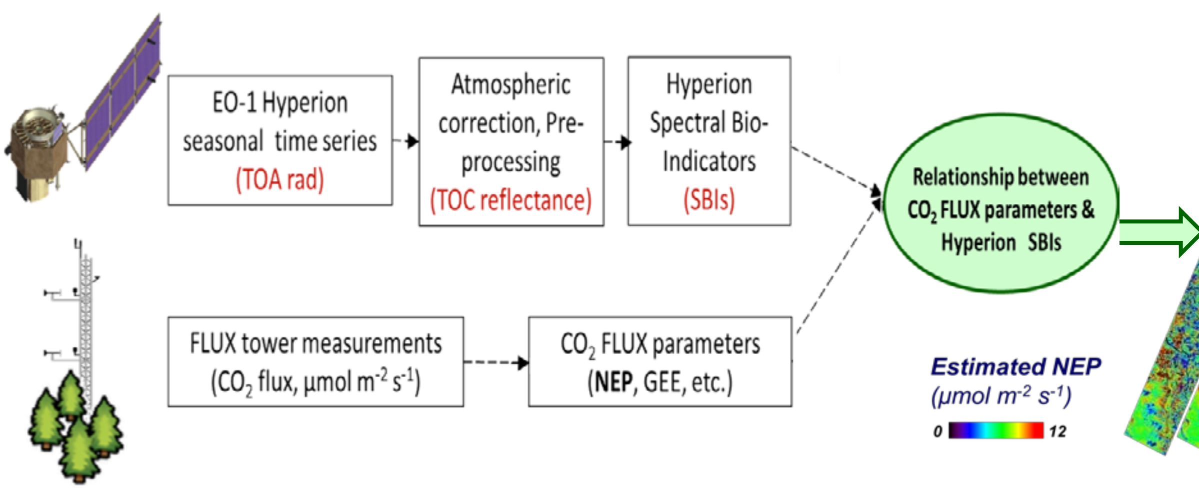

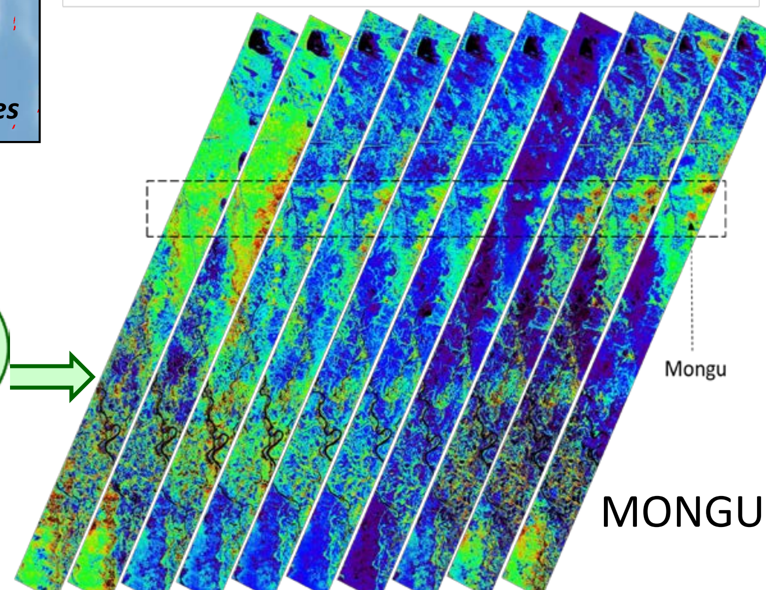

Campbell, Huemmrich, and Middleton

Midday GEP vs. APAR

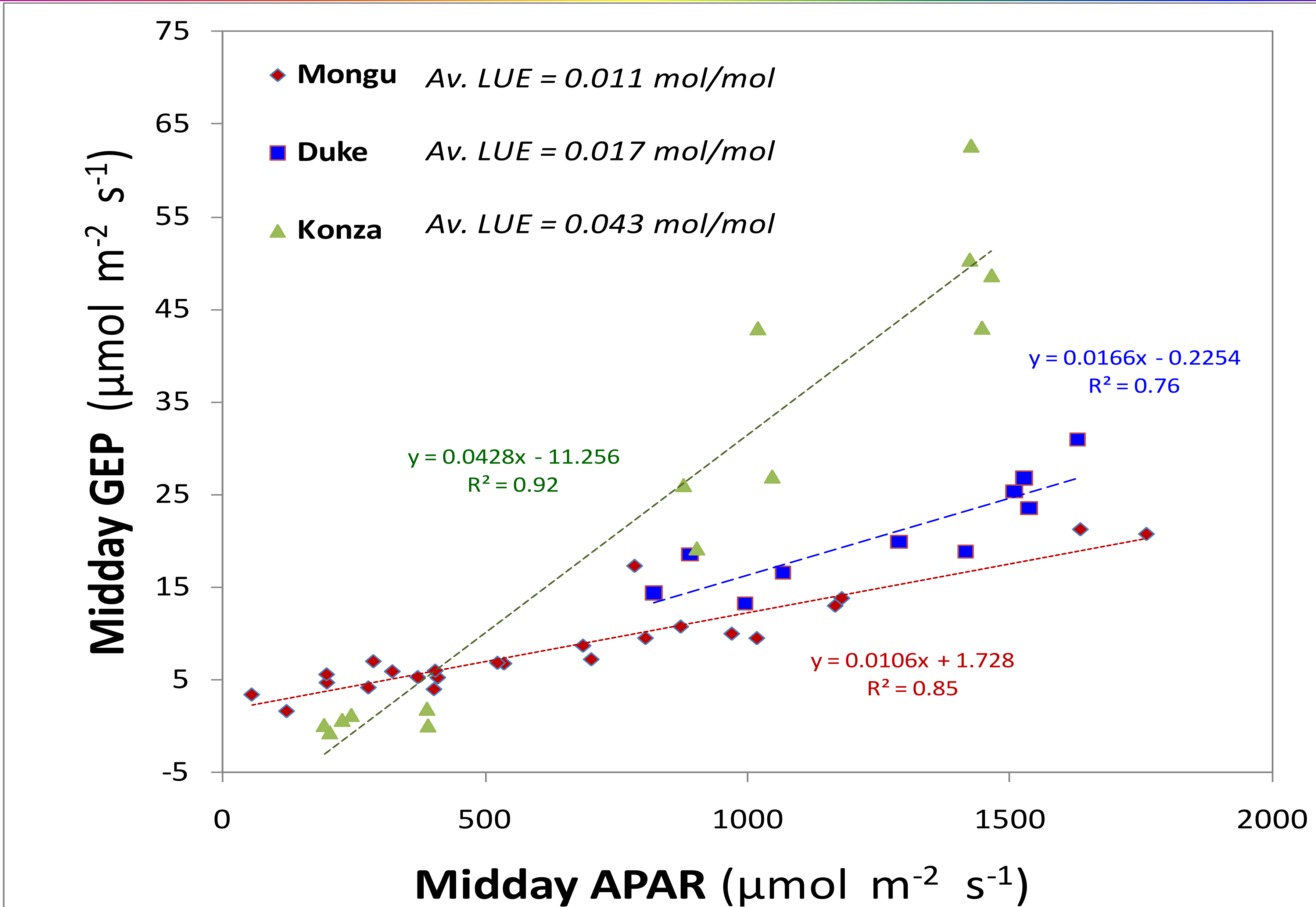

Hyperion Chlorophyll (and LAI) VIs and GEP

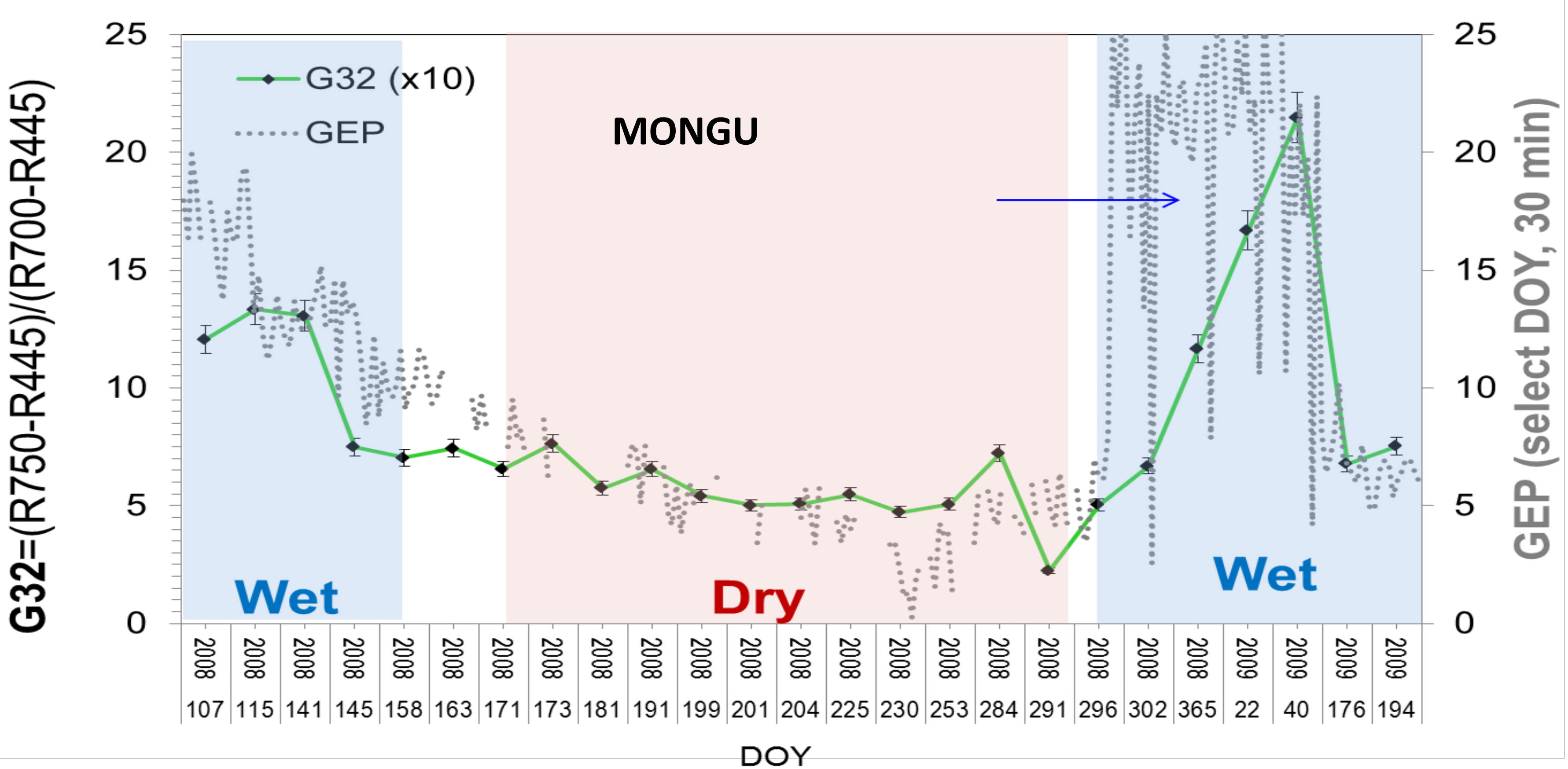

DOY

The spectral bio-indicator associated with chlorophyll content (G32, green line) tracing the CO_2 dynamics related to vegetation phenology

Spatial Distribution Maps, Capturing the Seasonal Range of CO_2 Absorbed by the Vegetation

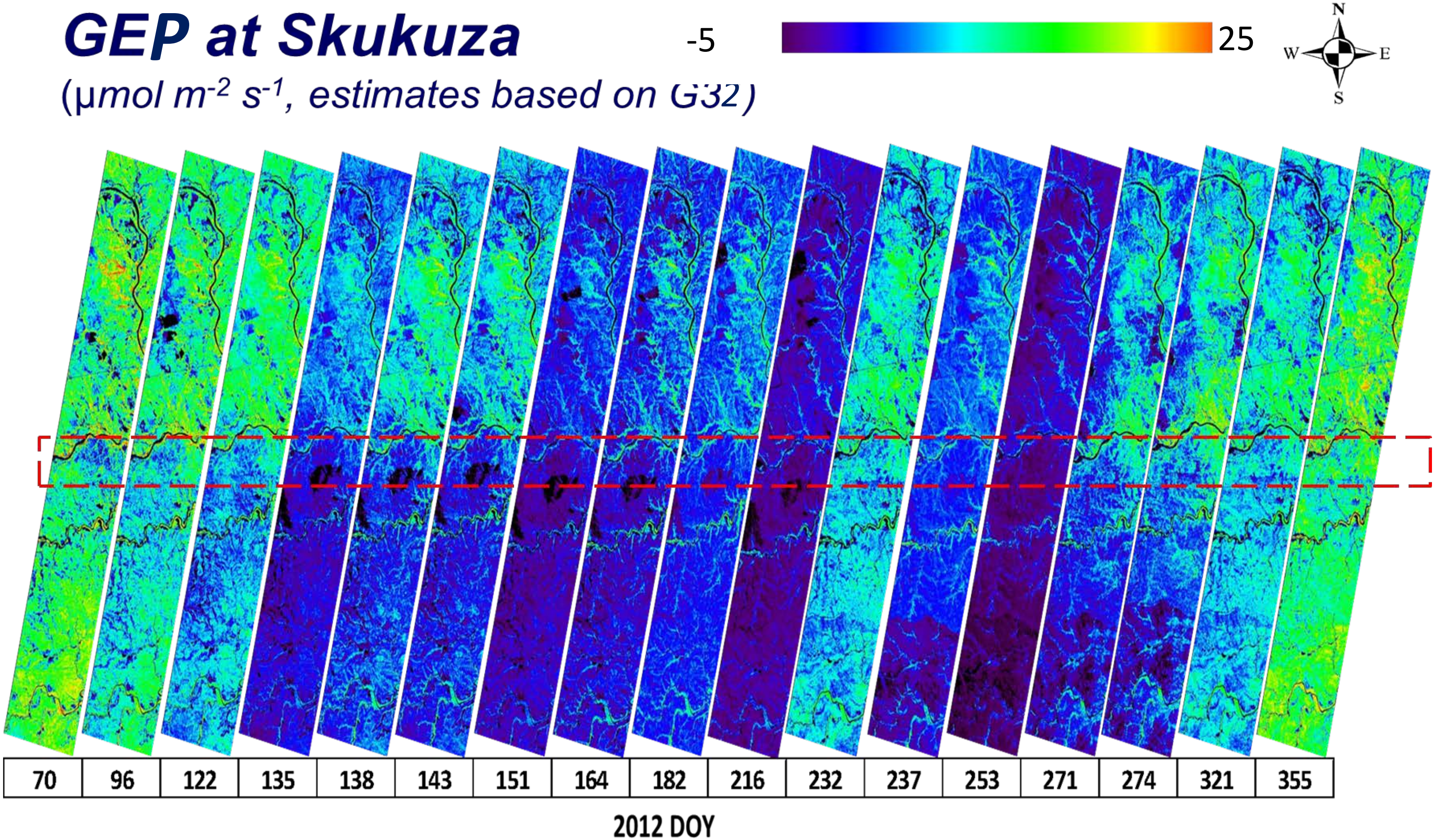

Hyperion's VIs associated with GPP are related to a suite of bio-physical parameters

Example for Skukuza (ZA-Kru)

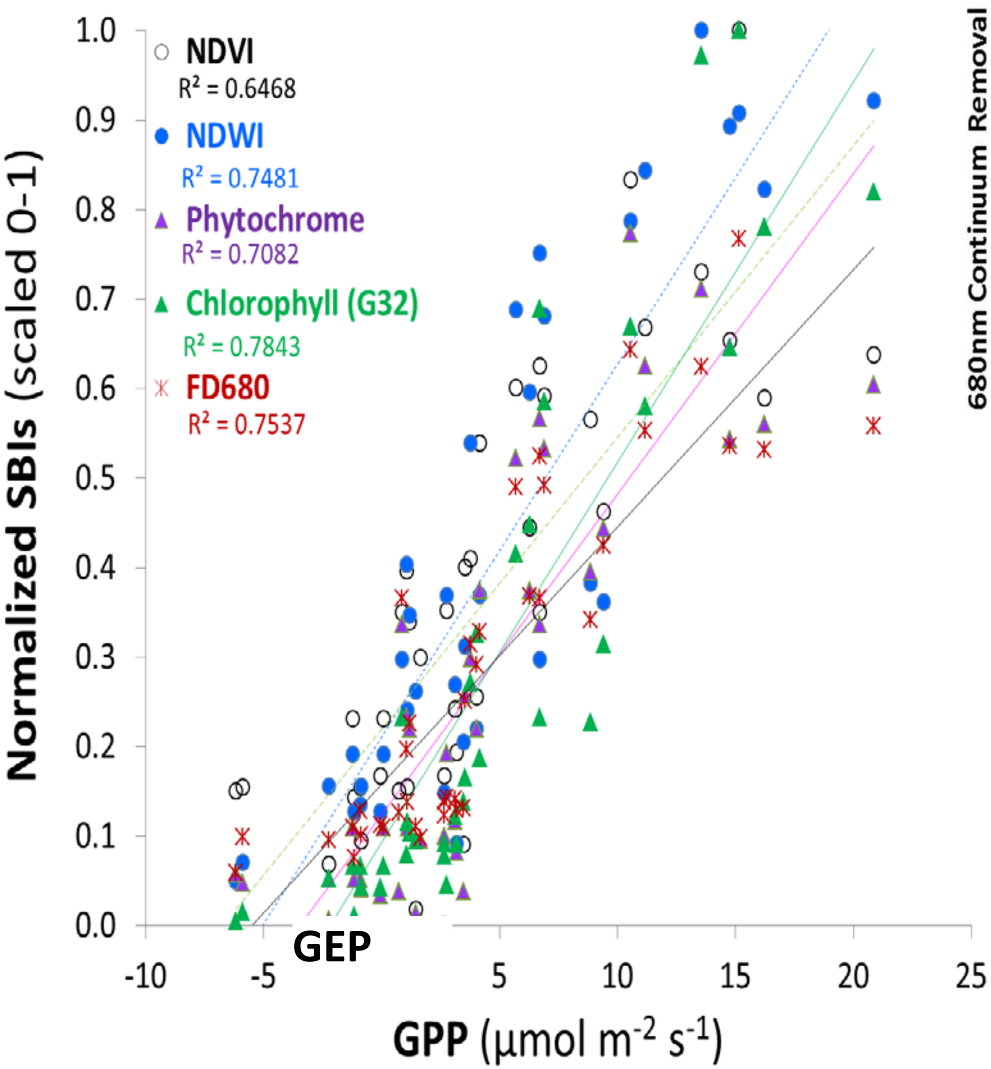

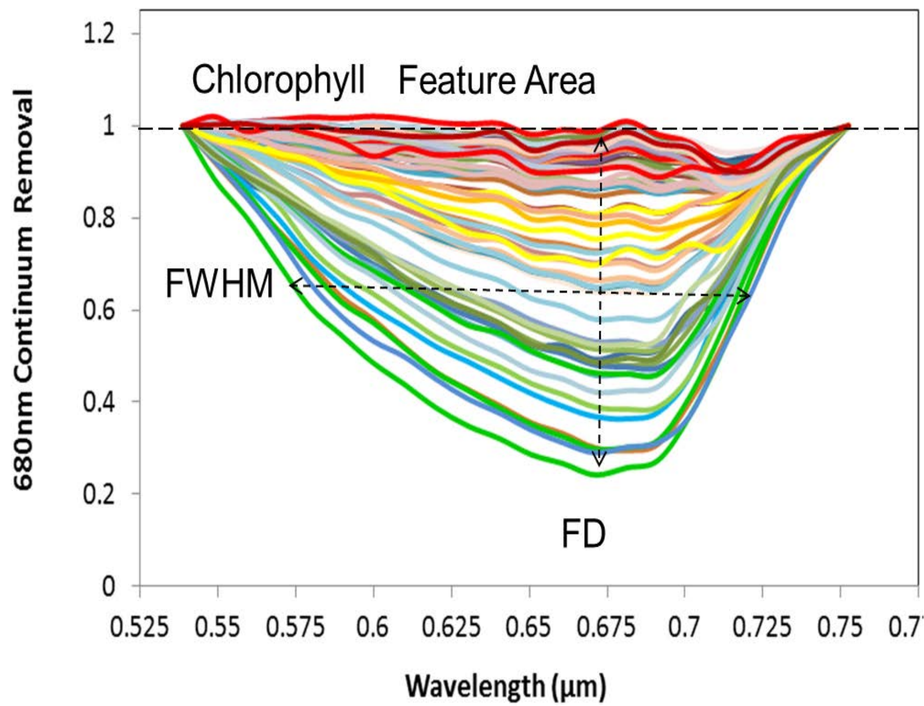

Spectral Parameters	R^2 to GEP
FD680 (PRISM)	0.75 *
FA680 (PRISM)	**0.82 ***
Phyt=(R724-R654)/(R724+R654)	0.71
G32=(R750-R445)/(R700-R445)	0.78 *
NDWI=(R819-R1649)/(R819+R1649)	0.74
NDVI=(TM4-TM3)/(TM4+TM3)	0.65

Midday GEP using a PLSR model at Skukuza

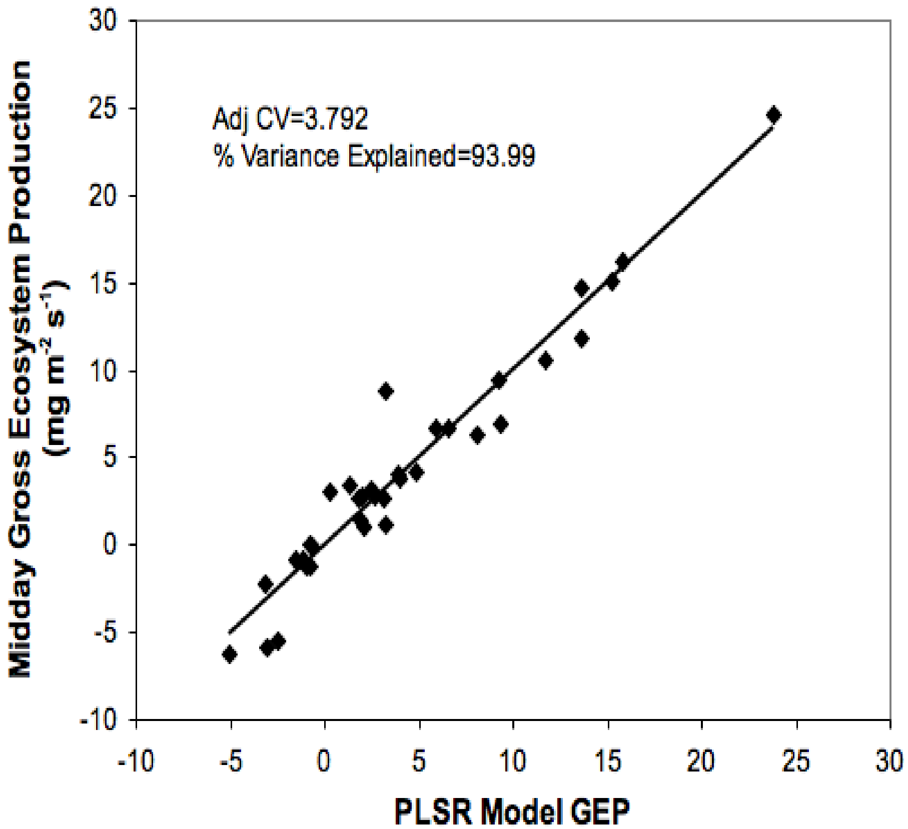

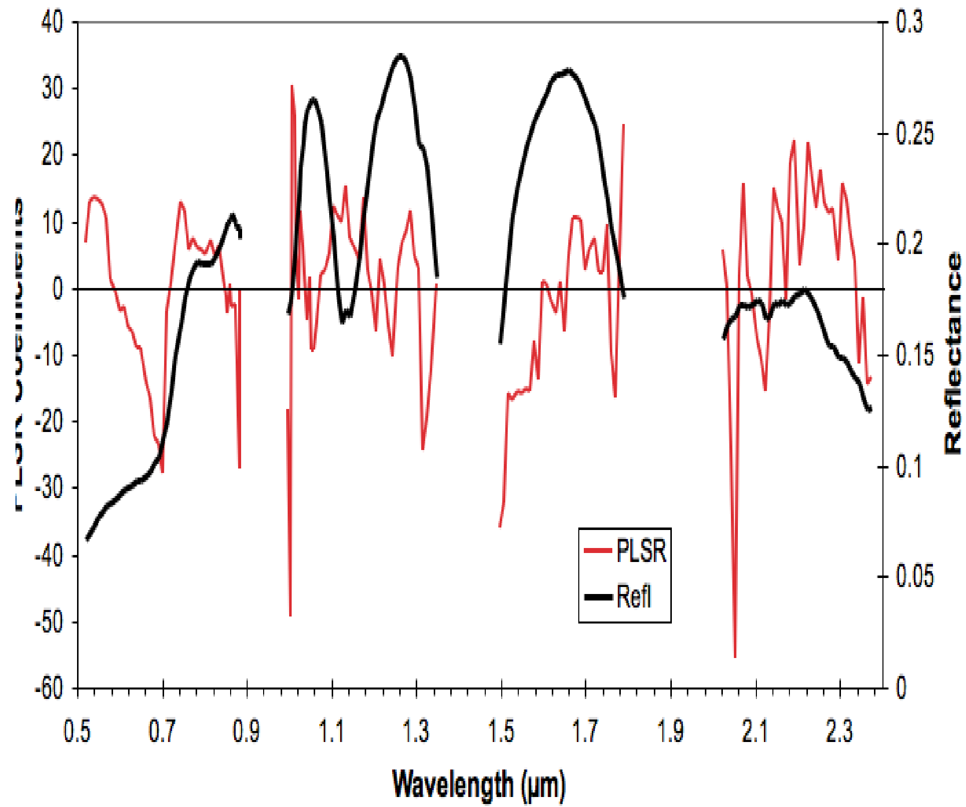

Average Hyperion spectral reflectance for Skukuza (black) and the coefficients derived from PLSR vs. Wavelength (red)

Midday GEP using a PLSR model at Howland, ME

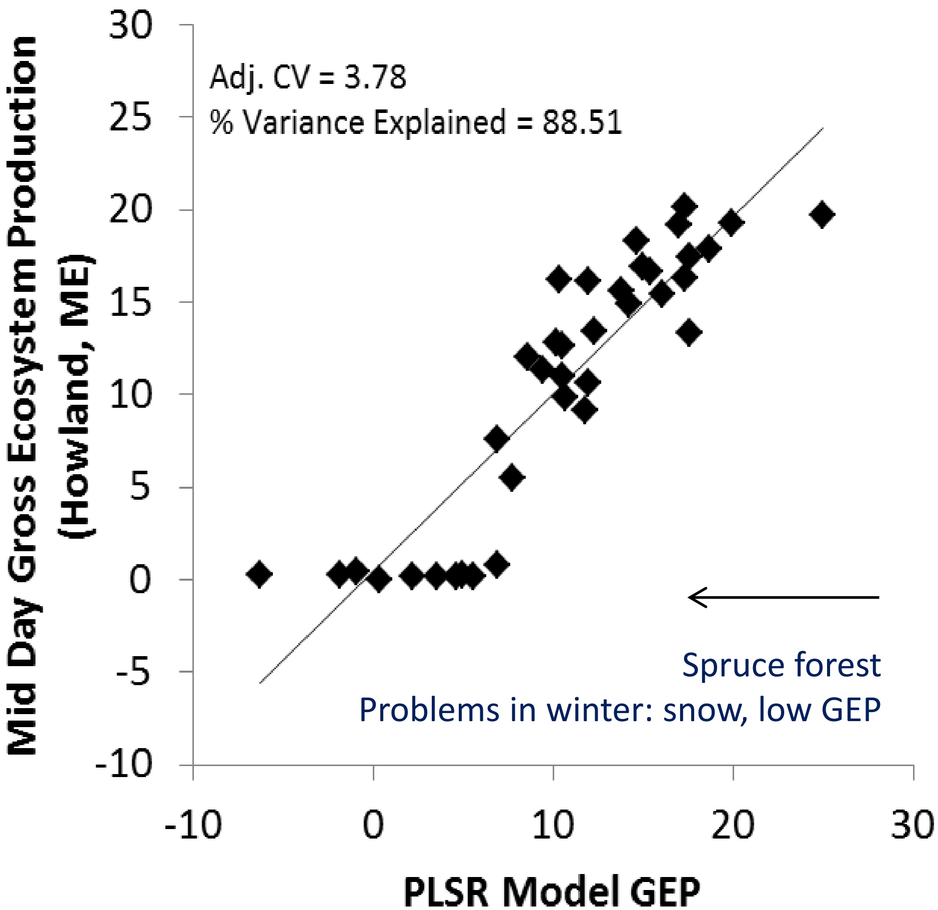

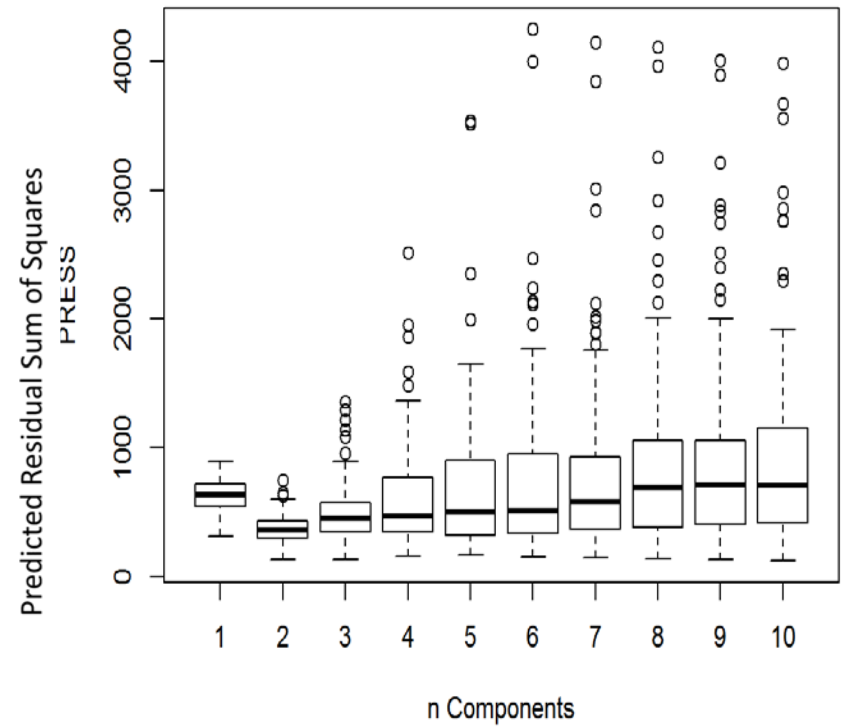

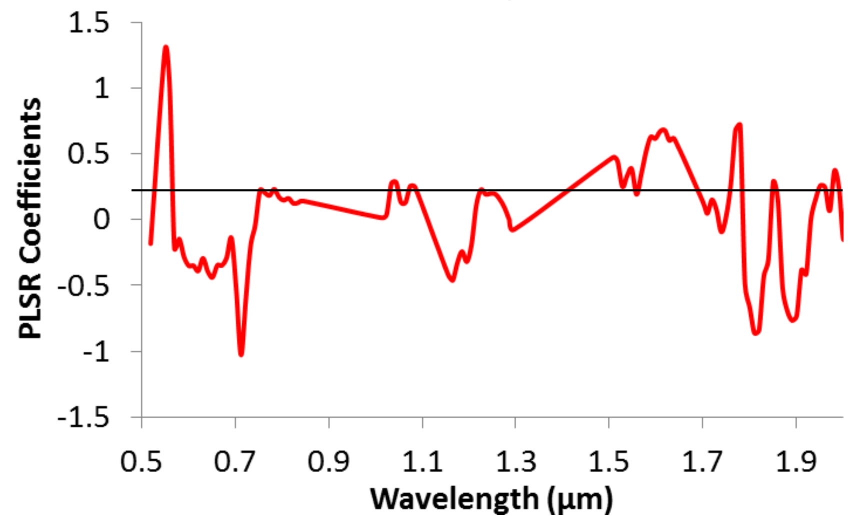

Hyperion reflectance PLSR components (black, top) and the coefficients derived from PLSR vs. Wavelength (red, below)

HyspIRI Studies of Ecosystem Processes and Characteristics: C4 Grassland Fraction

Utilize EO-1 Hyperion's spectral information to describe distributions of key plant functional types

C3 and C4 plants differ in leaf anatomy and enzymes used in photosynthesis. These differences are important as they determine optimal growing conditions, nitrogen and water-use efficiency, and seasonal growth patterns.

The Konza Prairie in Kansas is a region where there is a range in the relative abundance of C3 and C4 plants, and that abundance varies with location and time of year. Species ground coverage is measured every year for different Konza watersheds.

Partial least squares regression of Hyperion spectra is able to describe C4 cover fractions for different Konza watersheds collected in different years.

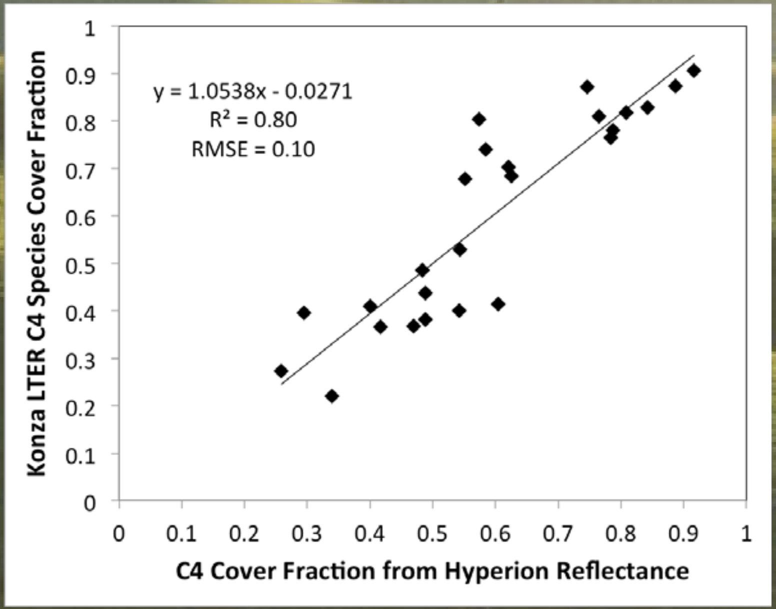

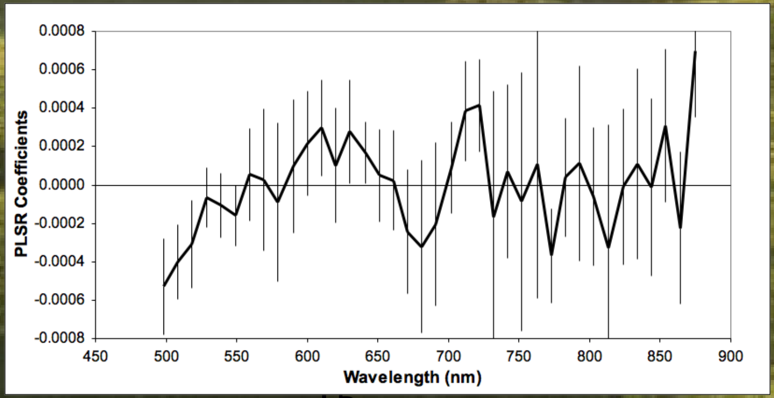

Huemmrich, Campbell, and Middleton

Modeling Canopy Bio-physical Parameters Hyperion's Reflectance and RTMo

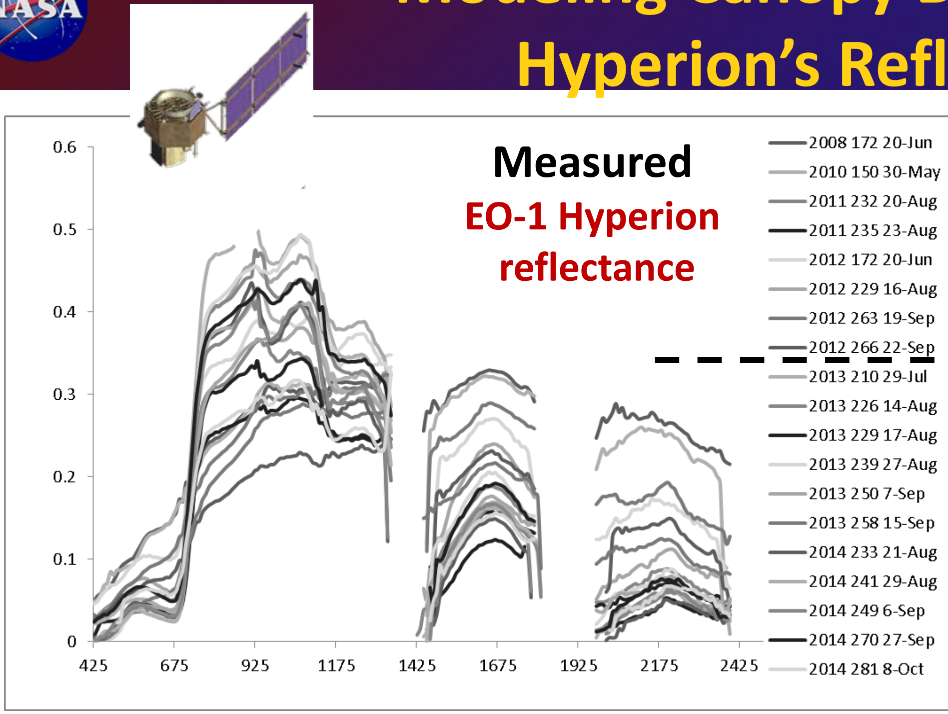

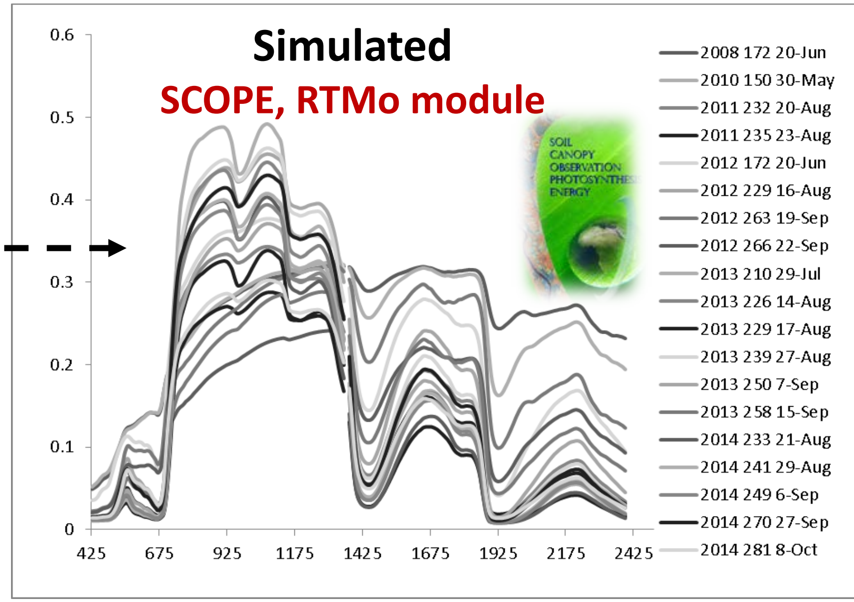

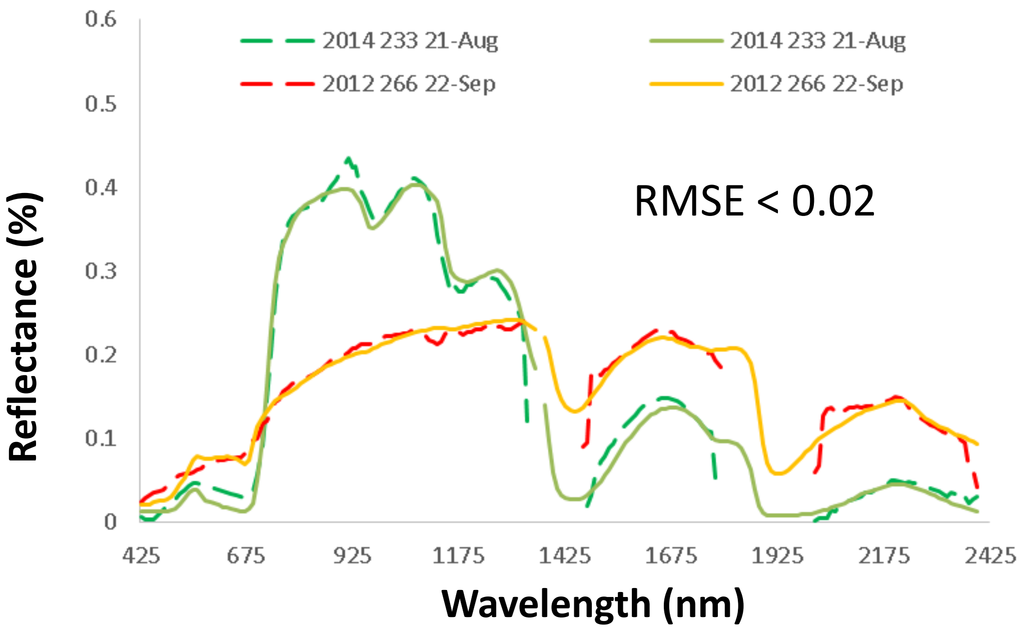

RTMo (part of SCOPE) includes:

- ***4SAIL - radiative transfer***
- ***Fluspect' - leaf optical***
- ***GSV - soil reflectance***

Hyperion Spectra Over a Cornfield

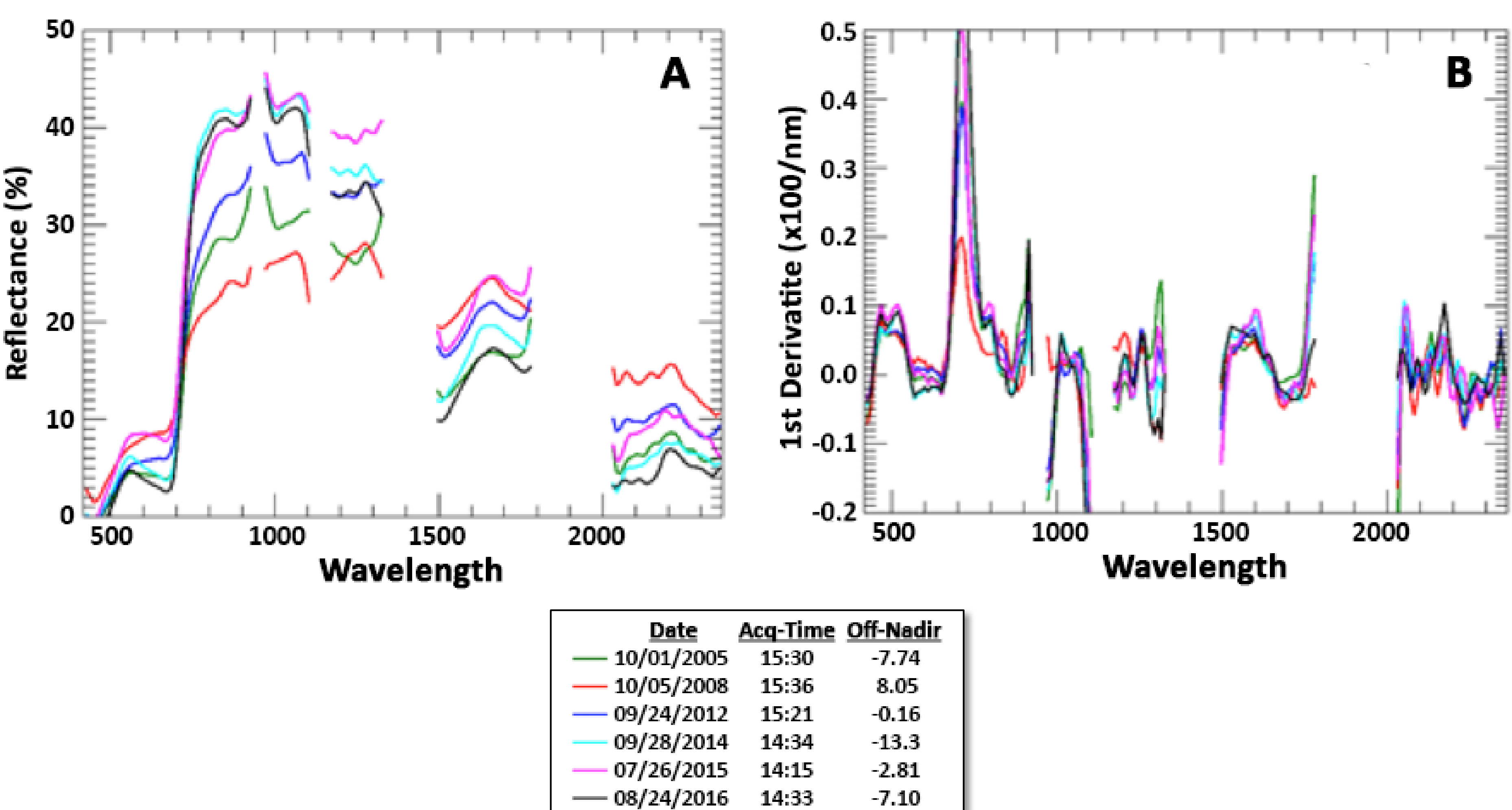

Hyperion spectra collected over a cornfield on six dates between 2005 and 2016, representing typical monthly data between July and October in any year: [A] original reflectance spectra; and [B] first derivative spectra of reflectance.   Frank et al., RS, 2017

Monitoring Ecosystem Gross Primary Production (GPP) with Space-Based, Hyperspectral Sensors

Qingyuan Zhang et. al., RSE, 2017.

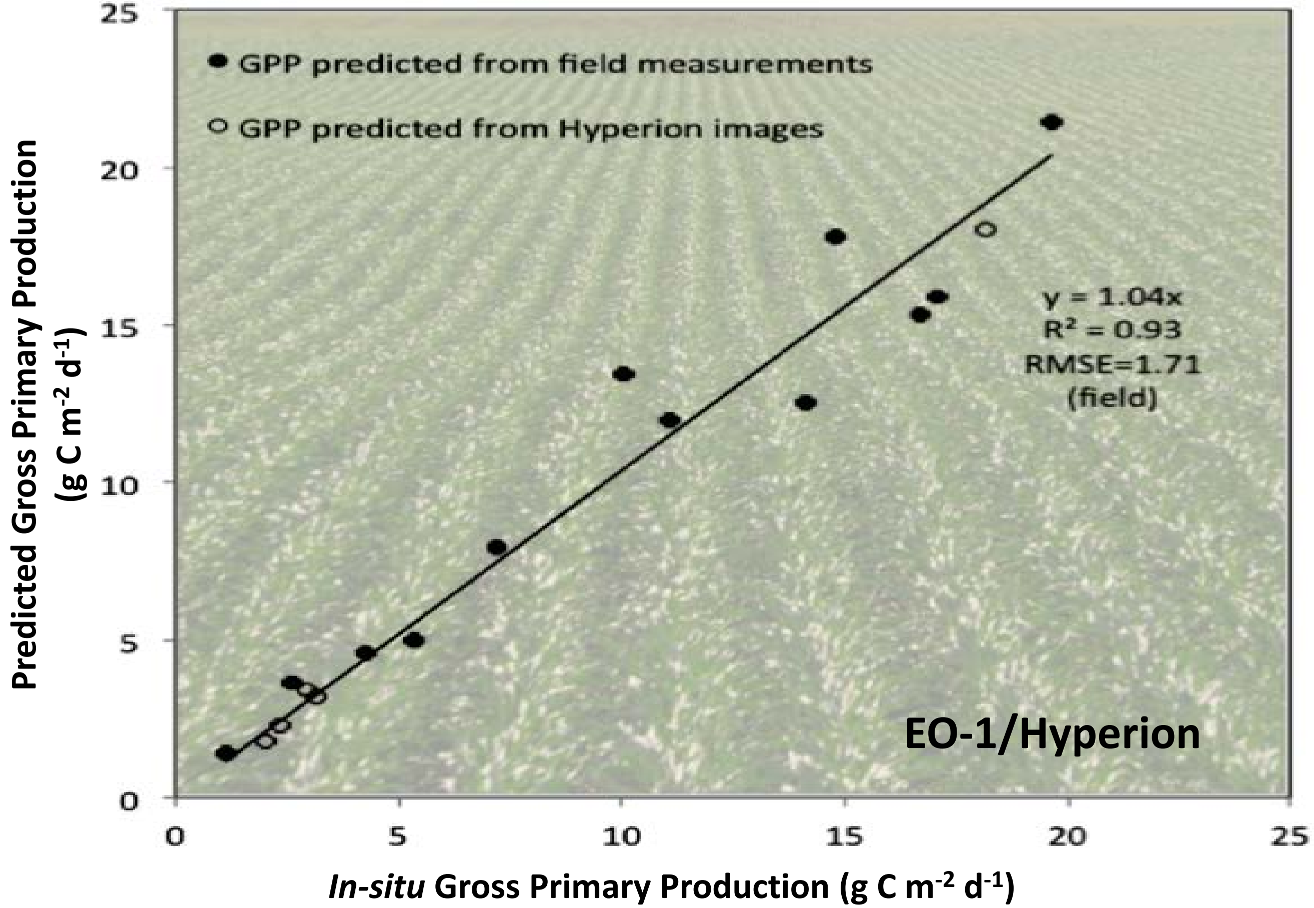

Based on Photochemical Reflectance Index, PRI

We demonstrate the capacity to monitor ecosystem Gross Primary Production (GPP) with both ground and space-based visible through shortwave infrared (VSWIR) spectrometers such as NASA's soon to be decommissioned EO-1/Hyperion and the future Hyperspectral Infrared Imager (HyspIRI) mission.

MODIS Retrievals of Gross Primary Production using the Photochemical Reflectance Index (PRI)

Middleton et al., RSE, 2016.

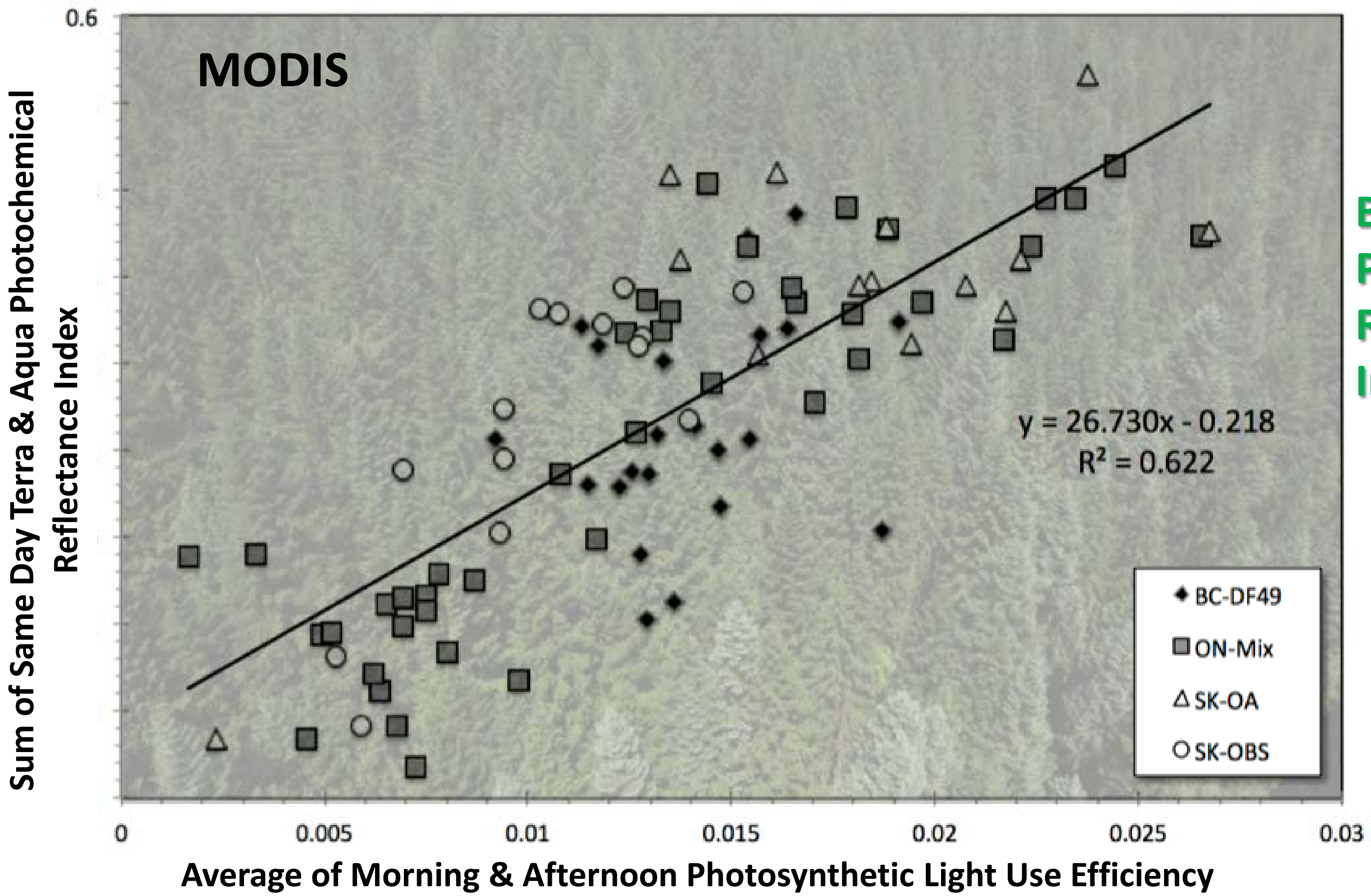

Based on Photochemical Reflectance Index, PRI

MODIS narrow ocean bands are used over land to monitor stress responses that inhibit carbon uptake in Canadian forest ecosystems. This study highlights the additional value of off-nadir directional reflectance observations along with the pairing of morning and afternoon satellite observations to improve retrievals of photosynthetic light use efficiency.

Diurnal Hysteresis Observed with SIF688 & PRI

Parker Tract Tower Site
Loblolly Pine: age class = 27-33 y

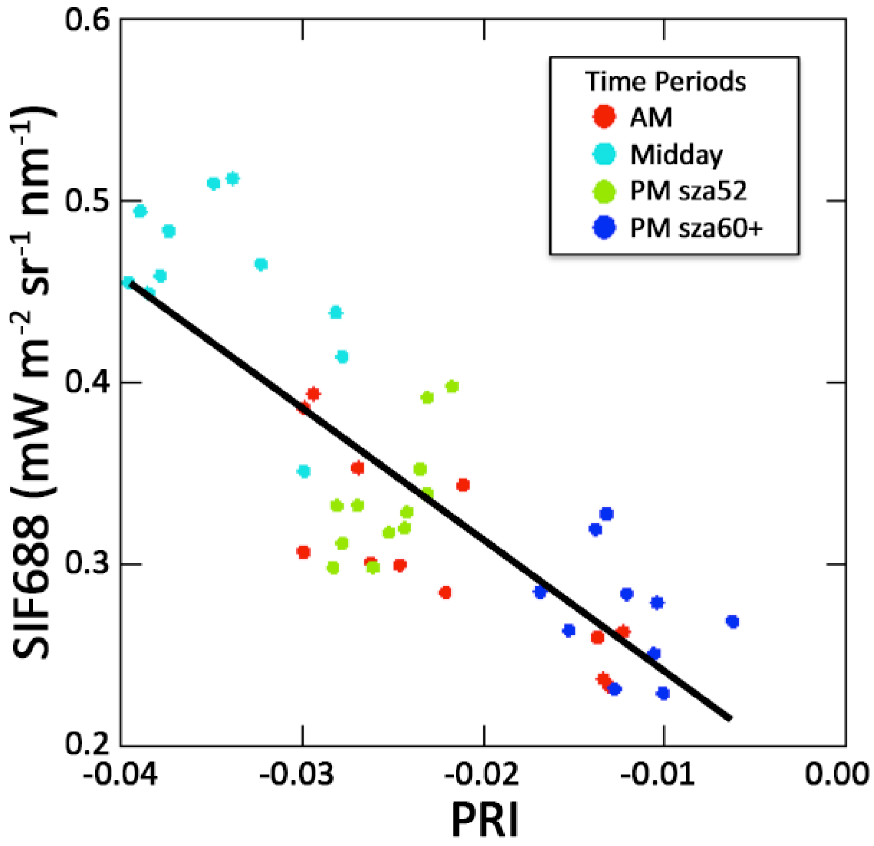

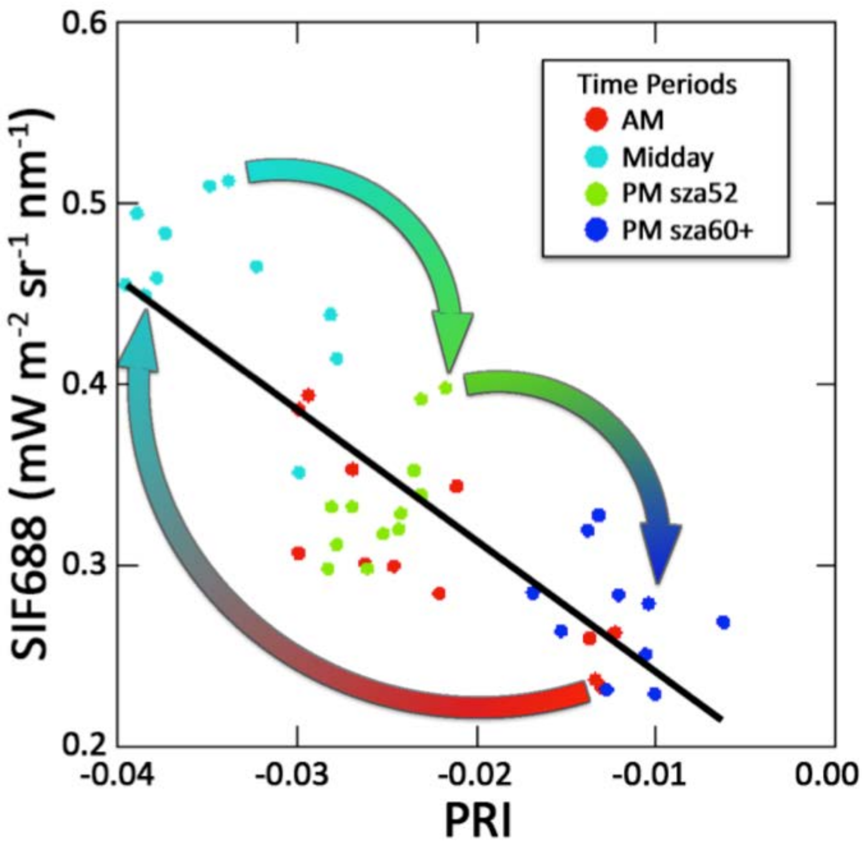

HyspIRI Studies of Ecosystem Processes and Characteristics: fAPARchl

Utilize EO-1 Hyperion's imaging spectroscopy for algorithm development and testing for new data products

30 m Hyperion Harvard, June 2008

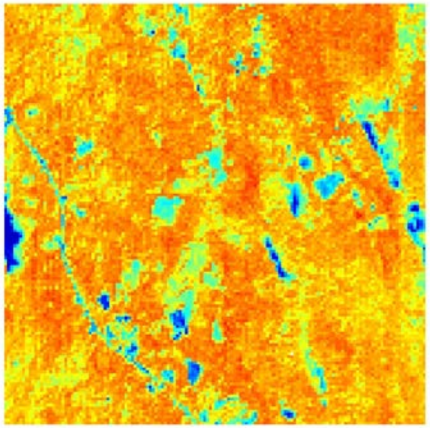

30 m Hyperion, Howland, June 2015

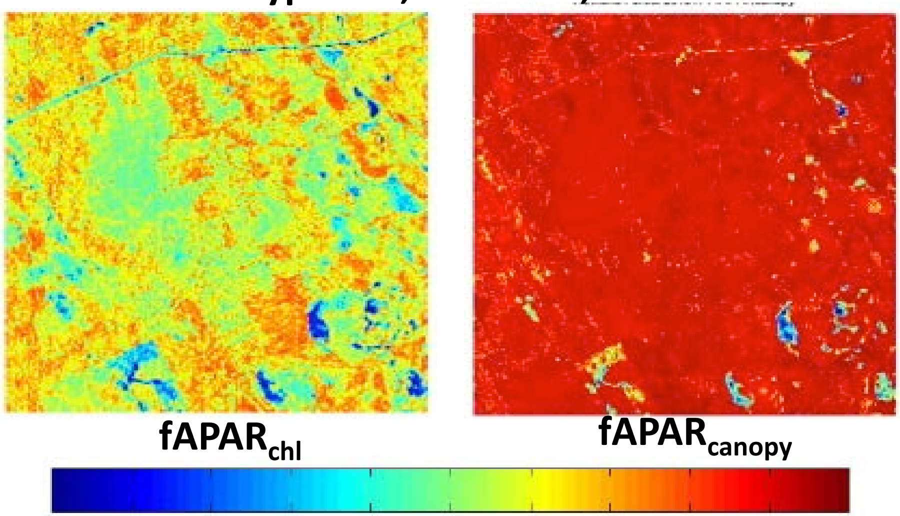

- Hyperion demonstrates accurate $fAPAR_{chl}$ for vegetation ($fAPAR_{chl}$ < $fAPAR_{canopy}$)

- Hyperion $fAPAR_{chl}$ = MODIS $fAPAR_{chl}$
- (30 m) (500 m)

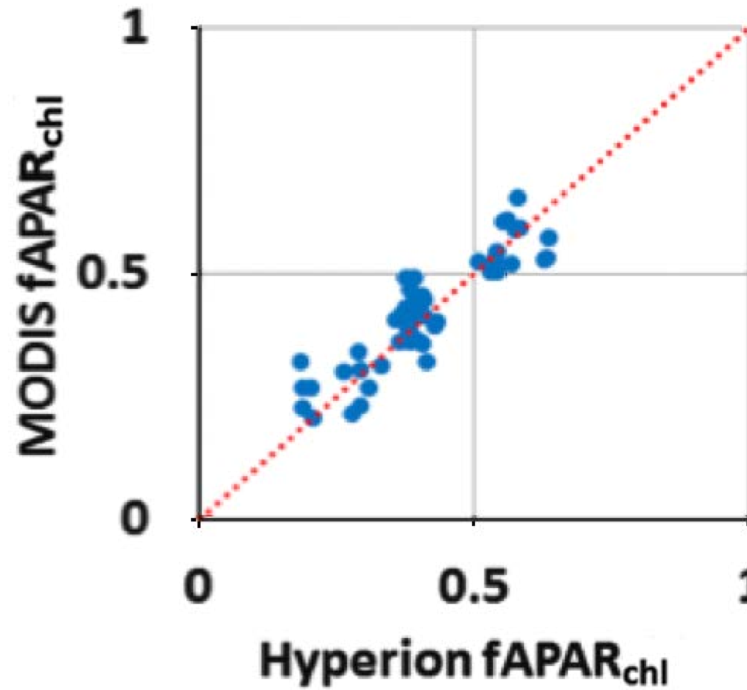

Zhang et al. 2012, 2013, 2014, 2016

HyspIRI Reflectance Time Series at Calibration Sites

Evaluating the consistency/stability of derived reflectance from Hyperion

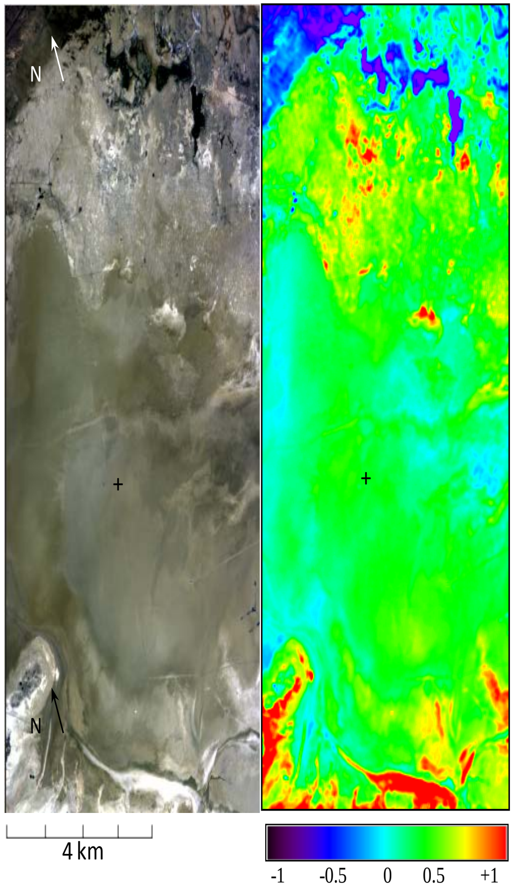

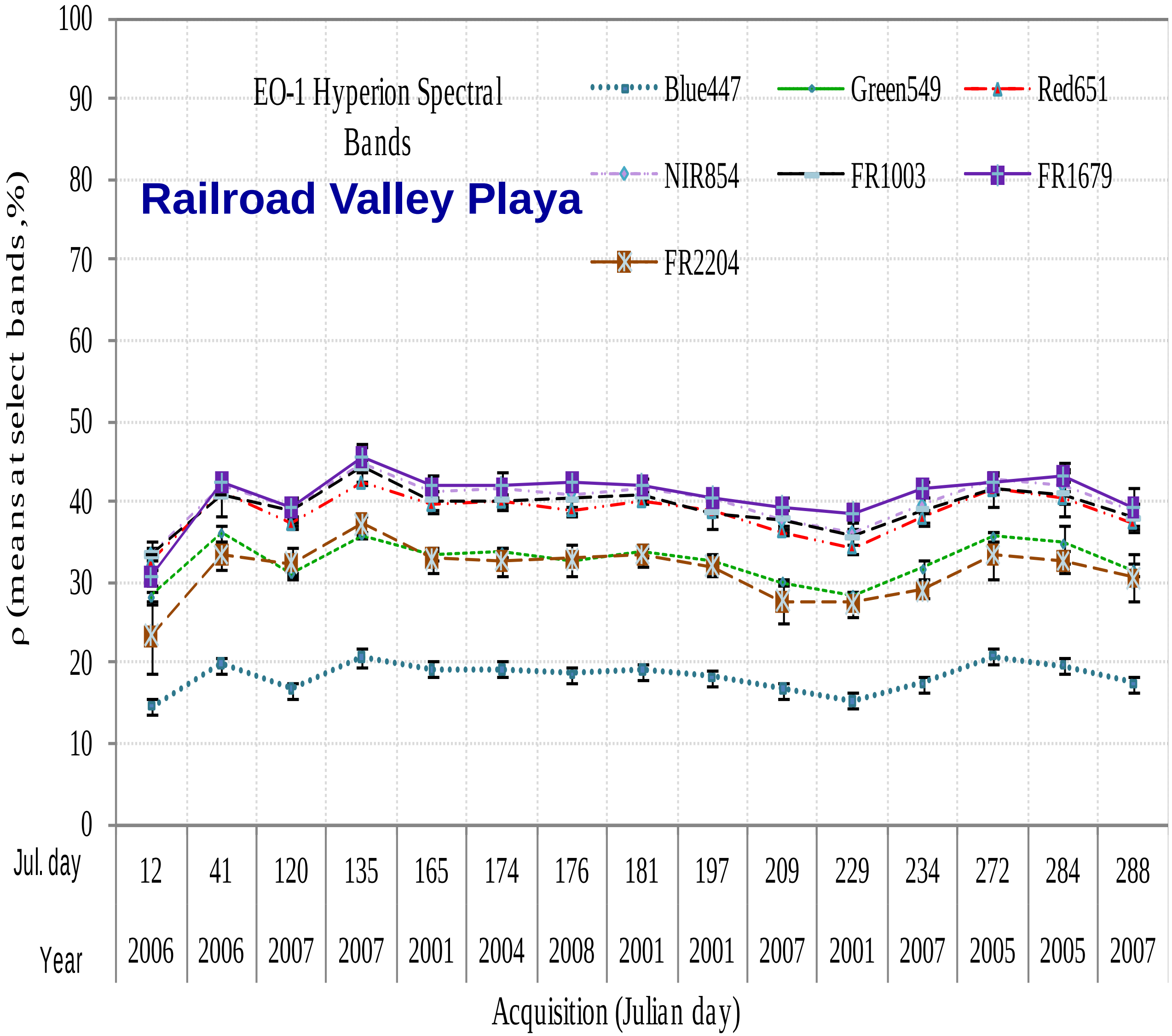

Hyperion VSWIR Over Libya-4

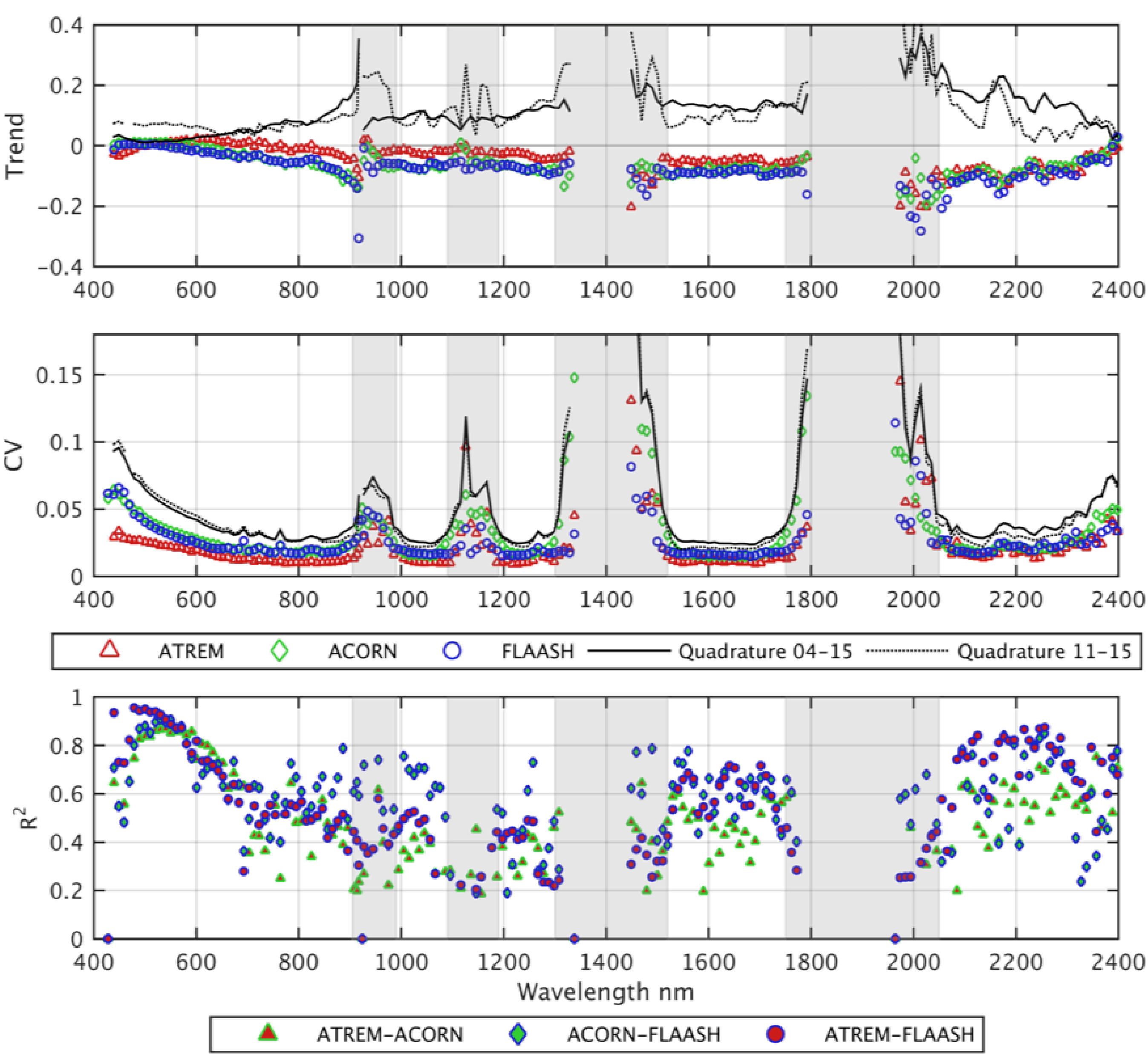

Top: Hyperion VSWIR surface reflectance of 35 images of Libya-4 acquired 2004-2015. Mean lifetime trends were determined with 3 atmospheric correction (AC) models; ATREM, ACORN, and FLAASH.

Middle: Temporal trend means across the spectrum, with the Q uncertainty estimate. Coefficient of variation trend for temporal trend, with Q.

Bottom: Coefficient of determination (R^2) between pairs of AC models, $p<0.01$.

Neigh et al. , GRSL, 2016

Coastal and Aquatic Products

Hyperion Reflectance of Apollo 16 Landing Site

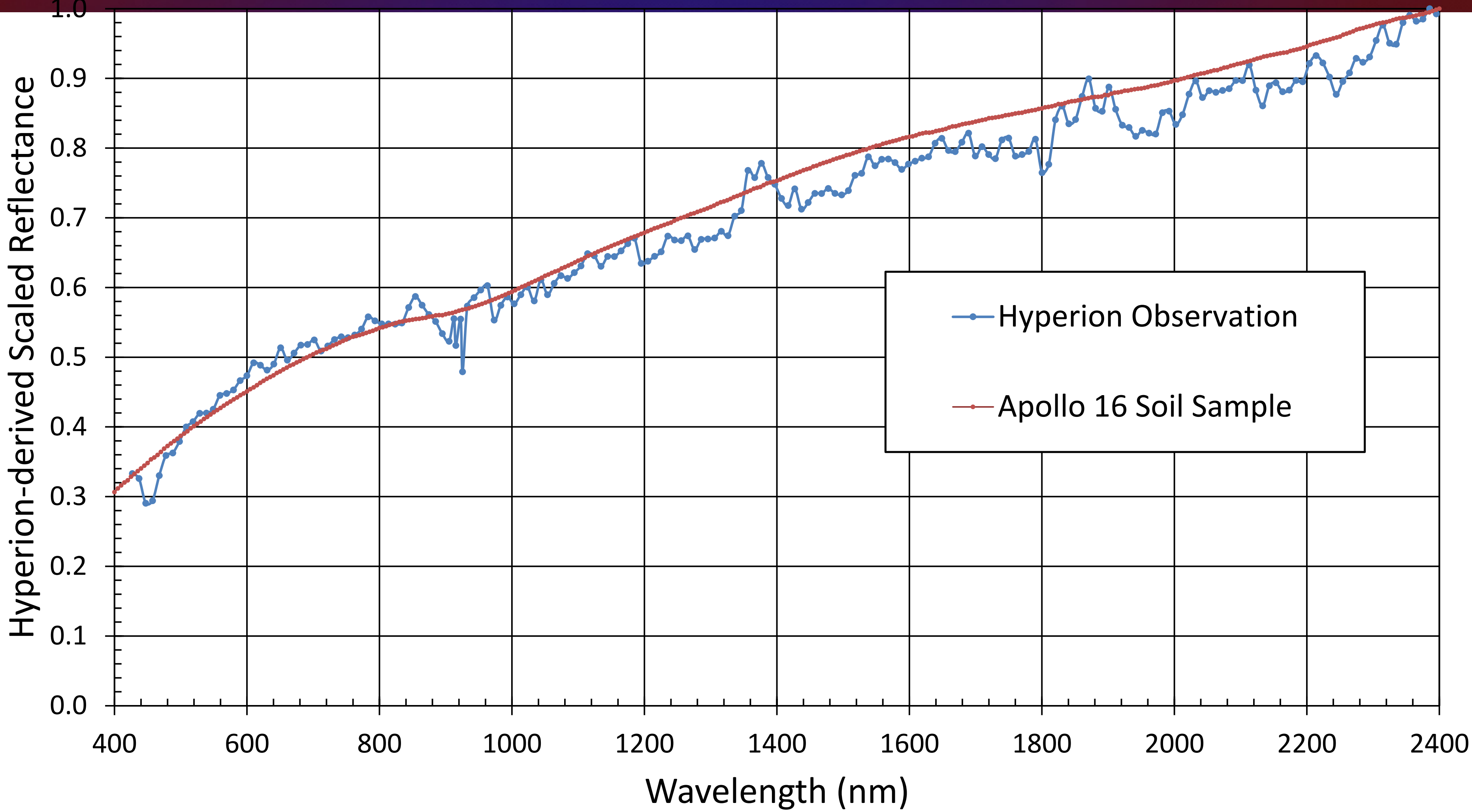

A comparison of Hyperion-derived reflectance with high resolution Apollo 16 soil sample spectra provided by the Lunar and Planetary Institute is shown.

GOME-2 SIF and APARchl

3 Years of GOME-2 & MODIS data

2008, 2010, 2012

over Nebraska, USA

GOME-2 2009 Annual Far-Red SIF

Reprocessed: Proof of Concept (AGU 2016)

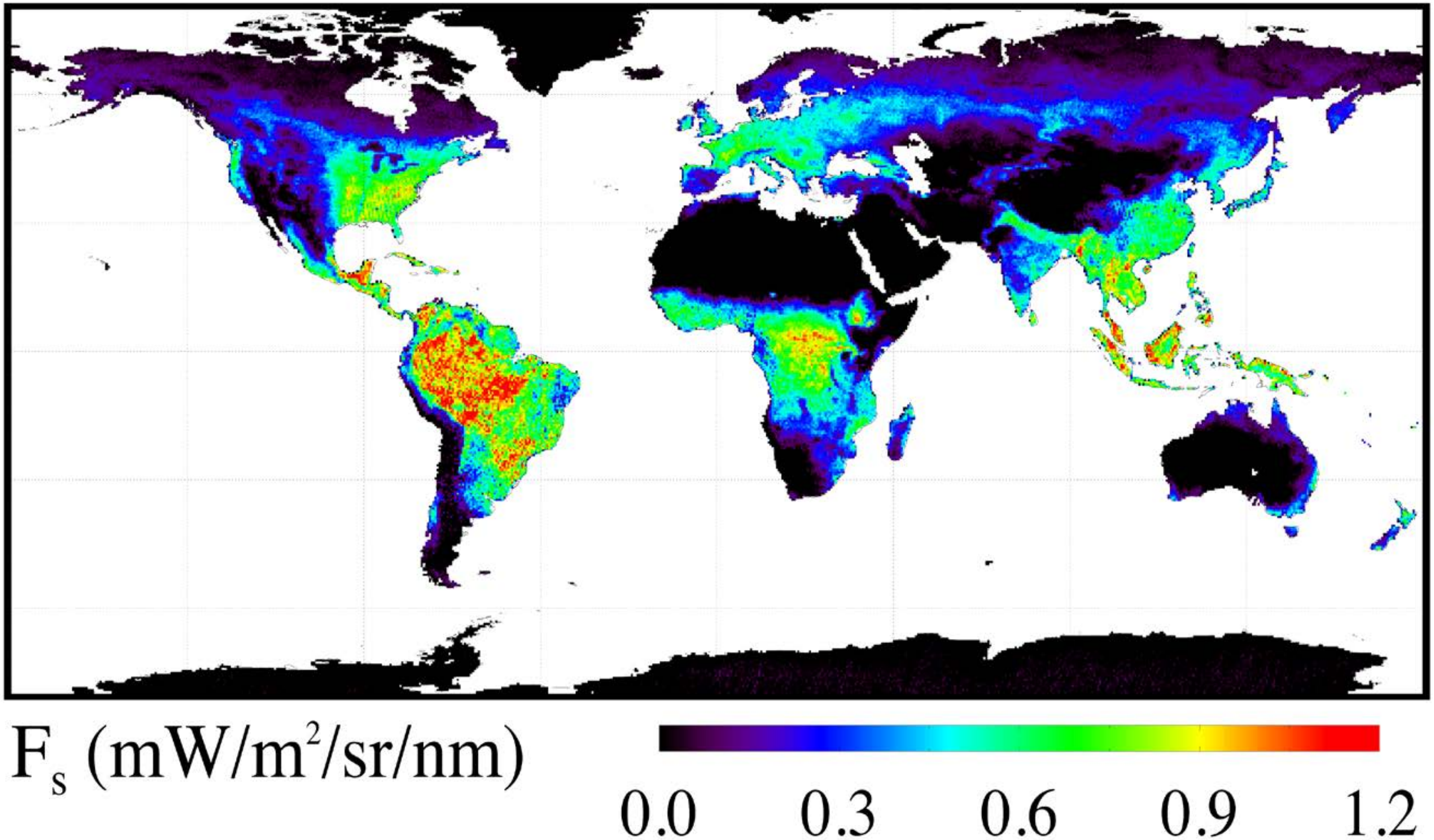

Joiner, J., Y. Yoshida, A. P. Vasilkov, Y. Yoshida, L. A. Corp, and E. M. Middleton (2011). First observations of global and seasonal terrestrial chlorophyll fluorescence from space, *Biogeosciences*, 8, 637–651, doi:10.5194/bg-8-637-2011.

Remote Sensing of fAPARchl

Traditional RTM and Indices	Advanced RTM PROSAIL4
Consider only Canopy and Soil	Distinguishes between **Canopy**, **Soil**, **Snow, and Surface Water**
Model needs plant functional type/land cover type as inputs for retrieval	Model *does not* need
Assumes that leaf optics of each type is fixed anywhere and anytime, and pre-determined.	Leaf optics are retrieved for each observation because leaf components change seasonally and spatially, even for same type.
MODIS bands 1 and 2 [Red, NIR]	MODIS bands 1 – 7 [5 VIS-NIR, 2 SWIR]
$fAPAR_{canopy}$	$fAPAR_{canopy}$, **$fAPAR_{chl}$** and $fAPAR_{non-chl}$

NDVI

NIR_V

EVI

NDSI

None of these distinguishes well between chlorophyll and non-chlorophyll components of vegetation, soil, open water, and snow, for a pixel.

Zhang, 2017

Common Reflectance Indices

$$NDVI = (\rho_{NIR1} - \rho_{red}) / (\rho_{NIR1} + \rho_{red})$$

$$NIR_V = \rho_{NIR1} \text{ X } NDVI$$

$$EVI = 2.5 \text{ X } [(\rho_{NIR1} - \rho_{red}) / (1 + \rho_{NIR1} + 6 \text{ X } \rho_{red} - 7.5 \text{ X } \rho_{blue})]$$

$$NDSI = (\rho_{green} - \rho_{SWIR1}) / (\rho_{green} + \rho_{SWIR1})$$

Remote Sensing of fAPARchl

Advanced Radiative Transfer Model PROSPECT+SAIL4 (PROSAIL4)

$fAPAR_{chl}$ and $fAPAR_{non\text{-}chl}$

$$fAPAR_{non\text{-}chl} = fAPAR_{brown\ pigment} + fAPAR_{dry\ matter} + fAPAR_{stem}$$

$$fAPAR_{canopy} = fAPAR_{chl} + fAPAR_{non\text{-}chl}$$

PAR – Photosynthetically Active Radiation (400 – 700 nm)

$$APAR_{chl} = fAPAR_{chl} \times \downarrow PAR$$

$$APAR_{canopy} = fAPAR_{canopy} \times \downarrow PAR$$

$$APAR_{canopy} \; (= fAPAR_{canopy} \times \downarrow PAR) >> APAR_{chl}$$

Zhang, 2017

References for fAPARchl

- Zhang, Q., et al. (**2005**), Estimating light absorption by chlorophyll, leaf and canopy in a deciduous broadleaf forest using MODIS data and a radiative transfer model, *Remote Sensing of Environment, 99*, 357-371.
- Zhang, Q., et al. (**2006**), Characterization of seasonal variation of forest canopy in a temperate deciduous broadleaf forest, using daily MODIS data, *Remote Sensing of Environment, 105*, 189-203.
- Zhang, Q., E.M. Middleton, et al. (**2009**). Can a satellite-derived estimate of the fraction of PAR absorbed by chlorophyll ($FAPAR_{chl}$) improve predictions of light-use efficiency and ecosystem photosynthesis for a boreal aspen forest? *Remote Sensing of Environment, 113*, 880-888.
- Zhang, Q., E.M. Middleton., B. Gao,. and Y. Cheng, (**2012**), Using EO-1 Hyperion to Simulate HyspIRI Products for a Coniferous Forest: The Fraction of PAR Absorbed by Chlorophyll (fAPAR(chl)) and Leaf Water Content (LWC), *IEEE Transactions on Geoscience and Remote Sensing, 50 (5)*, 1844-1852.
- Zhang, Q., E.M. Middleton, Y. Cheng. And D.R. Landis, (**2013**), Variations of Foliage Chlorophyll fAPAR and Foliage Non-chlorophyll fAPAR (fAPARchl, fAPARnon-chl) at the Harvard Forest, *IEEE Journal of Selected Topics on Applied Earth Observations and Remote Sensing, 6(5)*, 2254 - 2264.
- Cheng, Y.-B., et al. (**2014**), Impacts of light use efficiency and fPAR parameterization on gross primary production modeling, *Agricultural and Forest Meteorology, 189-190*, 187-197.
- Zhang, Q., et al. (**2014**), Estimation of crop gross primary production (GPP): $fAPAR_{chl}$ versus MOD15A2 FPAR, *Remote Sensing of Environment, 153*, 1-6.
- Zhang, Q., et al. (**2015**), Estimation of crop gross primary production (GPP): II. Do scaled MODIS vegetation indices improve performance?, *Agricultural and Forest Meteorology,* 200, 1-8.
- Zhang, Q., E.M. Middleton, et al. (**2016**), Integrating chlorophyll fAPAR and nadir photochemical reflectance index from EO-1/Hyperion to predict cornfield daily gross primary production, *Remote Sensing of Environment, 186, 311-321.*

2006 NLCD Map of 50x50km Area Around US-NE1

US-NE1

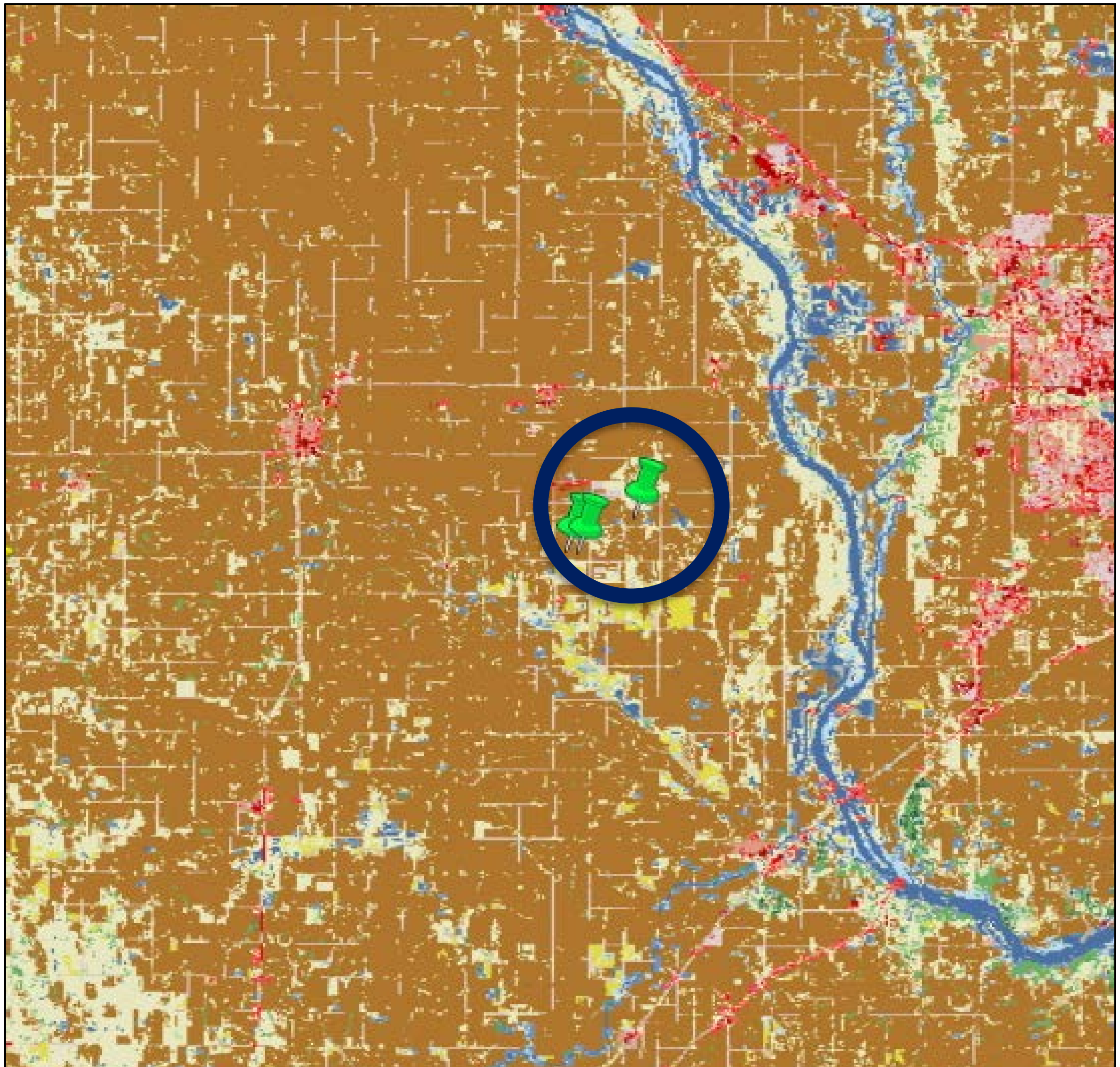

NLCD Land Cover Classification Legend

- 11 Open Water
- 12 Perennial Ice/ Snow
- 21 Developed, Open Space
- 22 Developed, Low Intensity
- 23 Developed, Medium Intensity
- 24 Developed, High Intensity
- 31 Barren Land (Rock/Sand/Clay)
- 41 Deciduous Forest
- 42 Evergreen Forest
- 43 Mixed Forest
- 51 Dwarf Scrub*
- 52 Shrub/Scrub
- 71 Grassland/Herbaceous
- 72 Sedge/Herbaceous*
- 73 Lichens*
- 74 Moss*
- 81 Pasture/Hay
- 82 Cultivated Crops √
- 90 Woody Wetlands
- 95 Emergent Herbaceous Wetlands

* Alaska only

Zhang, 2017

Data Sources

* Terra MODIS: MAIAC 8-day 500 m surface reflectance

$fAPAR_{canopy}$, $fAPAR_{chl}$ & $fAPAR_{non\text{-}chl}$ - bands 1 - 7

NDVI and NIR_V - bands 1, 2

EVI - bands 1, 2, 3

* GOME-2 (Global Ozone Monitoring Experiment -2)

SIF ($\lambda_{emission}$=740 nm), swath width 1920 km

Pixel spatial resolution (nadir): ~ 0.5°

Spectral resolution ~ 0.5 nm (S/N ~1000)

ftp://ftp.gfz-potsdam.de/home/mefe/GlobFluo/GOME-2/ungridded/

* Tower ↓PAR at US-Ne1

MODIS Products:
RGB, fAPARcanopy, fAPARchl, fAPARnon-chl, NDVI, & EVI

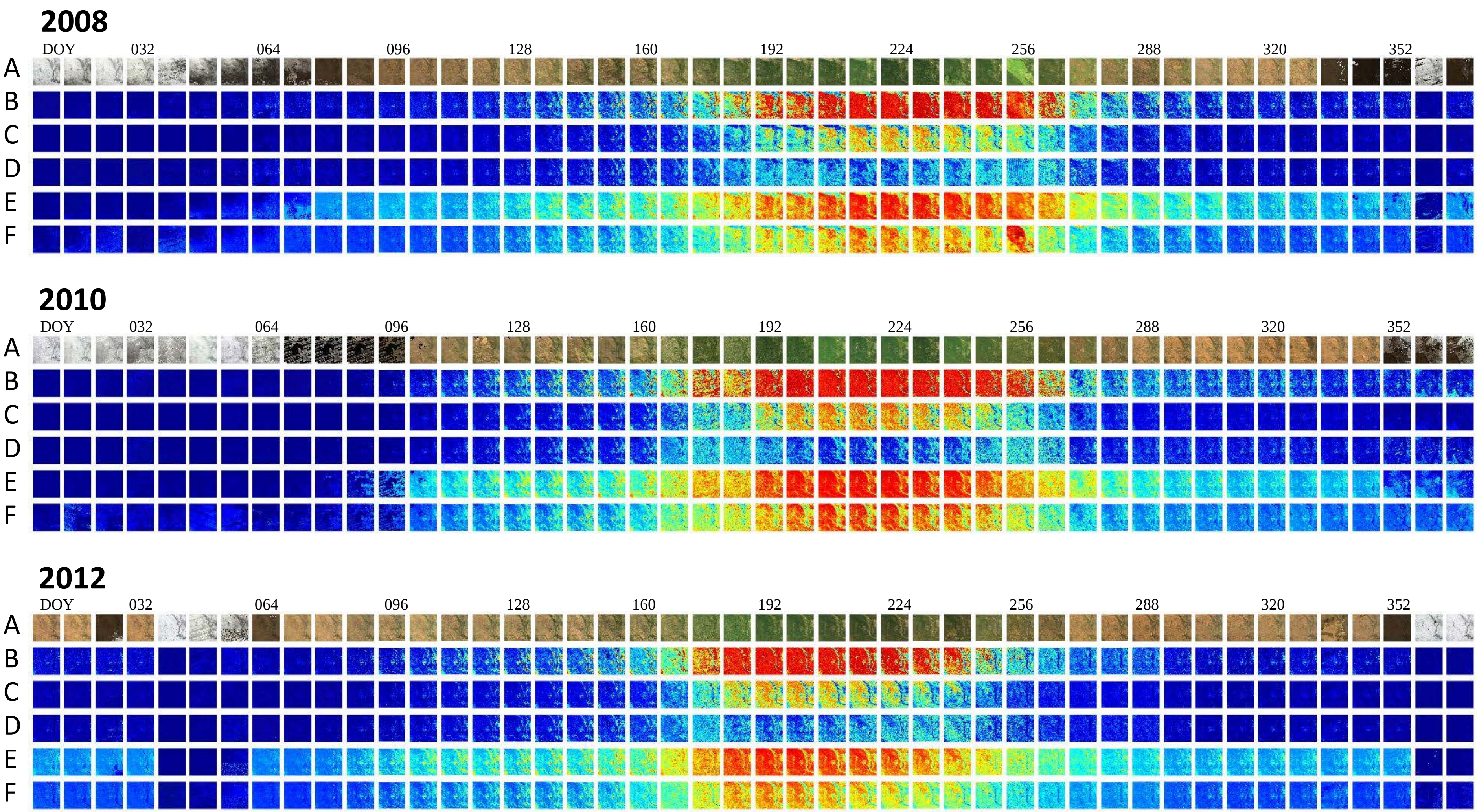

A: RGB image
B: fAPARcanopy
C: fAPARchl
D: fAPARnon-chl
E: NDVI
F: EVI

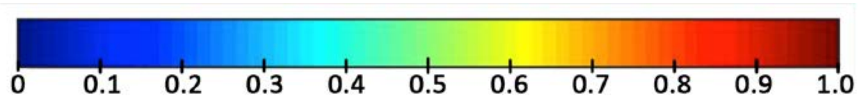

Zhang, 2017

fAPARchl Derived from MODIS

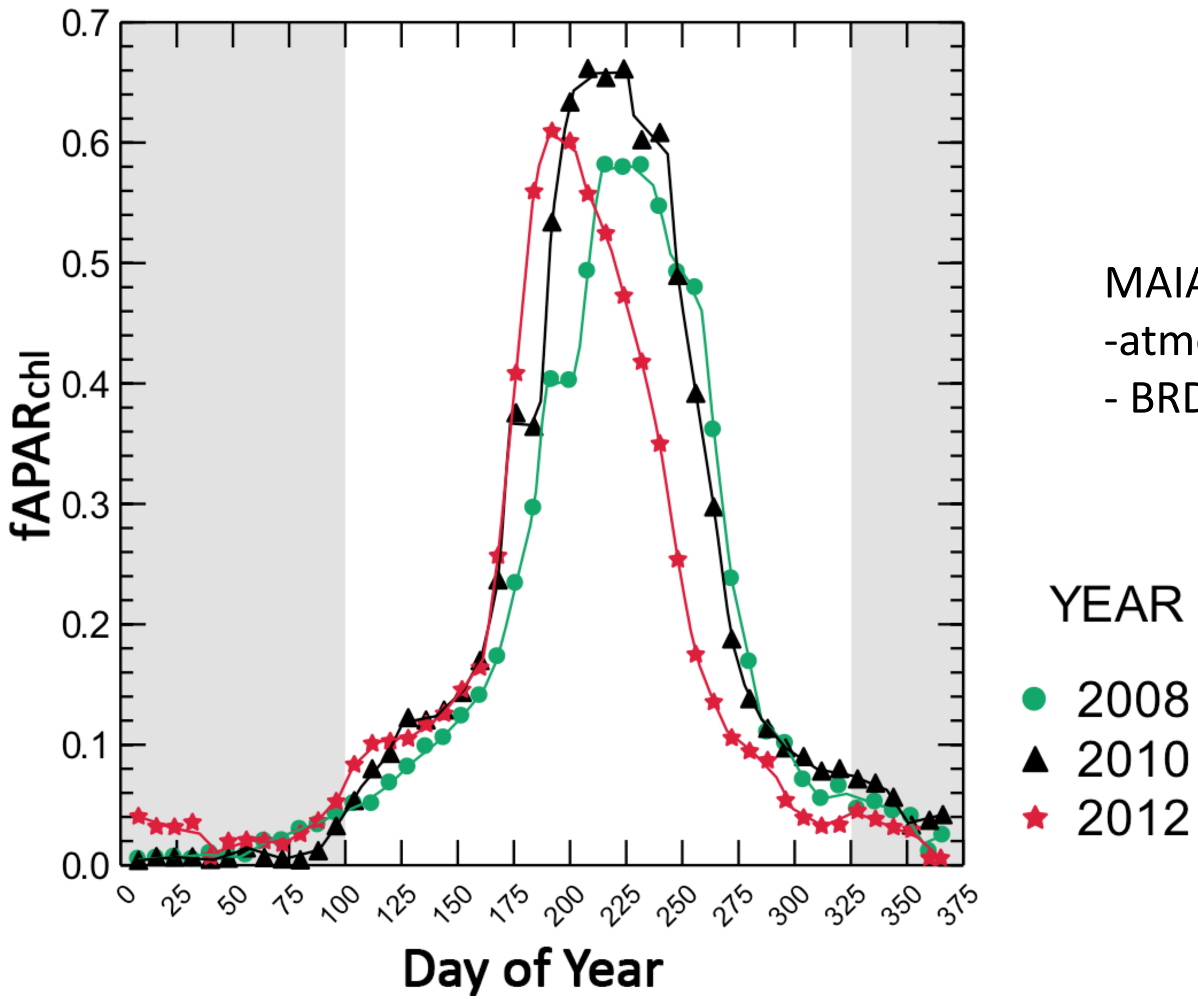

MAIAC corrected
-atmosphere
- BRDF

Annual patterns for 8-day averages of fAPARchl derived from MODIS in 3 years. Data represent 50 km x 50 km regions centered on the Nebraska research cornfield site (US-NE1). The “green period” is defined as DOYs 100 - 325 (SIF > 0).

APARchl Derived from MODIS & NE-1

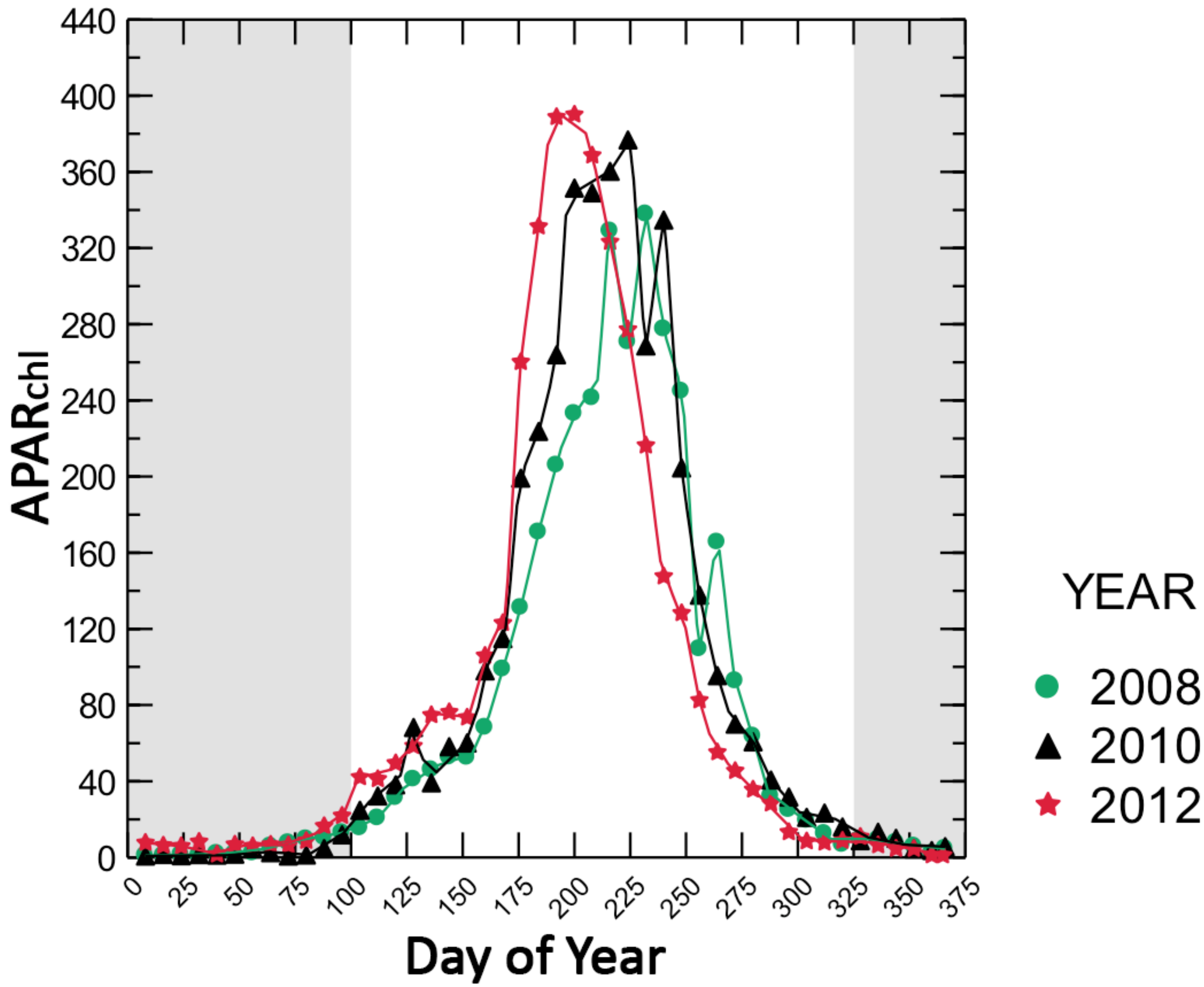

Annual patterns for 8-day averages of APARchl derived in 3 years from MODIS and from PAR measured at the NE-1 flux tower site (Meade, NE, USA). Data represent 50 km x 50 km regions centered on NE-1. The "green period" is defined as DOYs 100 - 325 (SIF > 0).

fAPARnon-chl

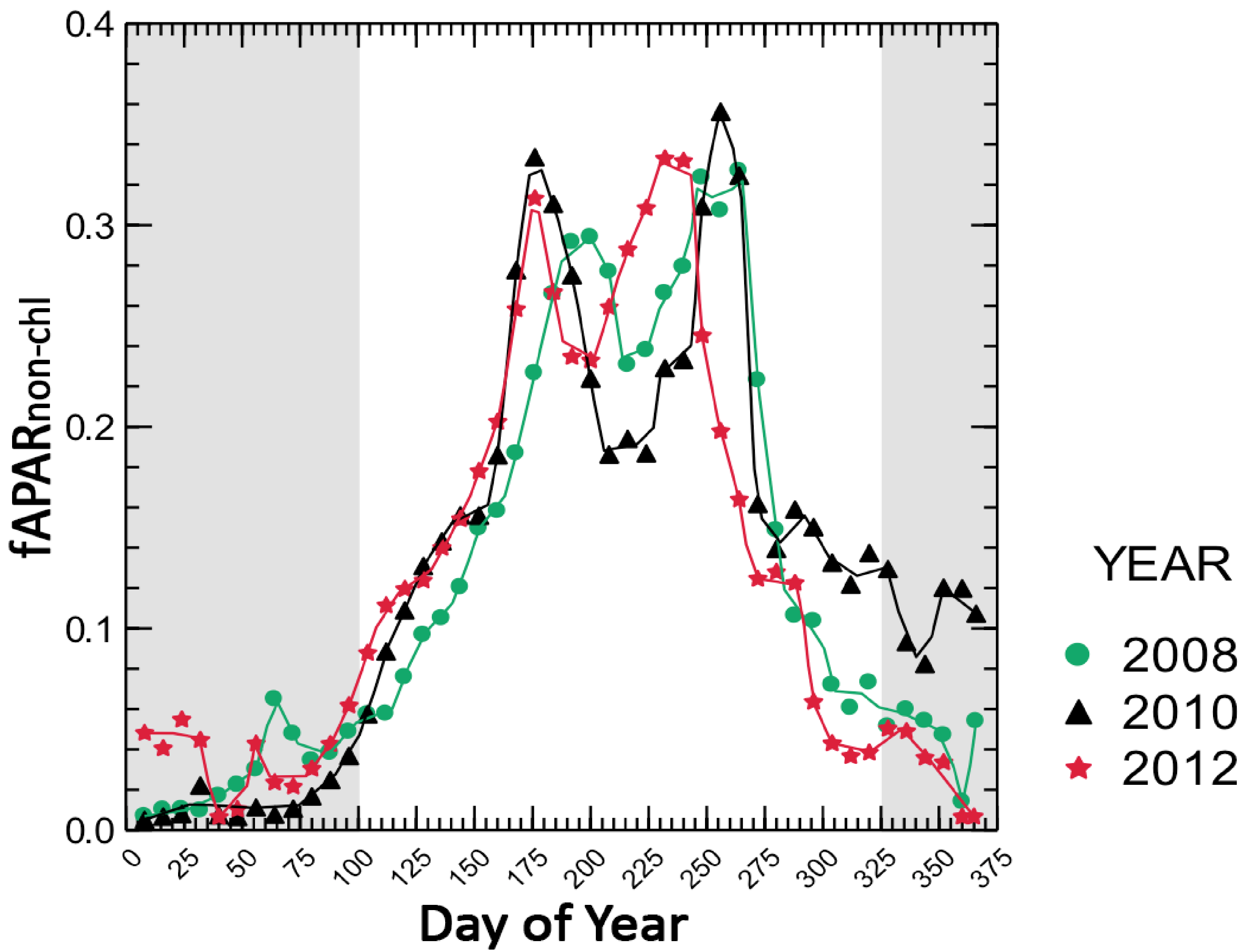

fAPARcanopy

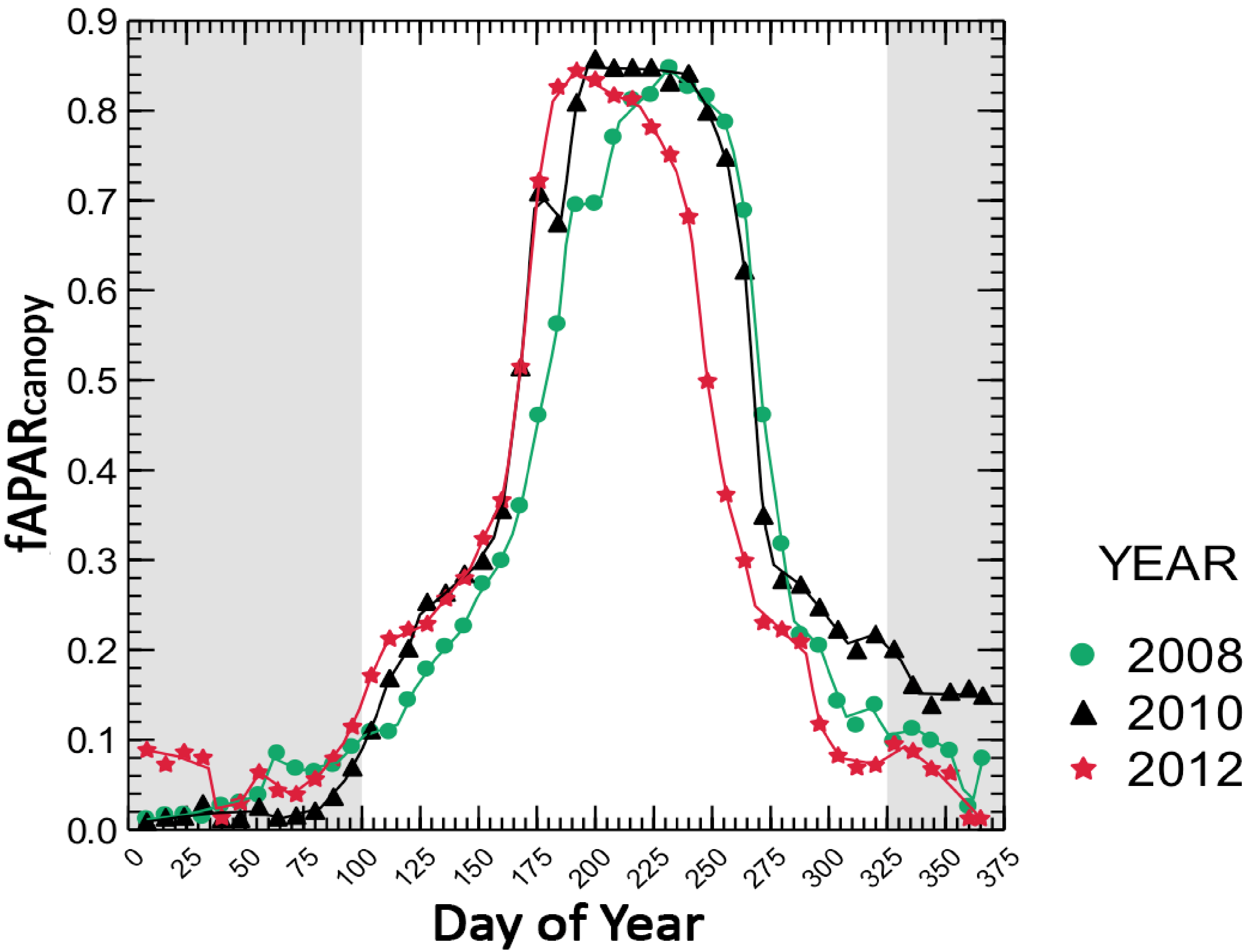

fAPAR variables & EVI vs. APARchl

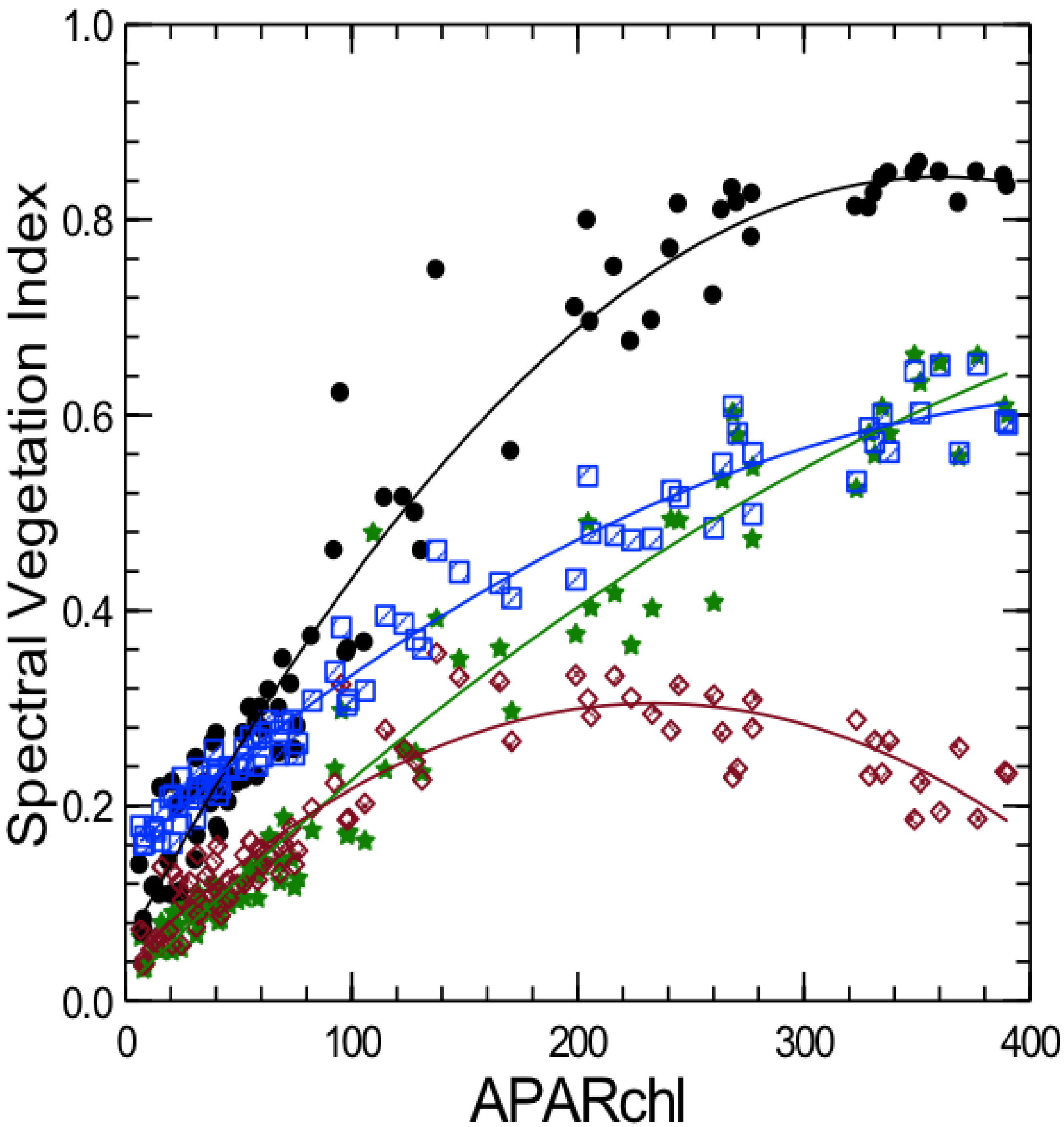

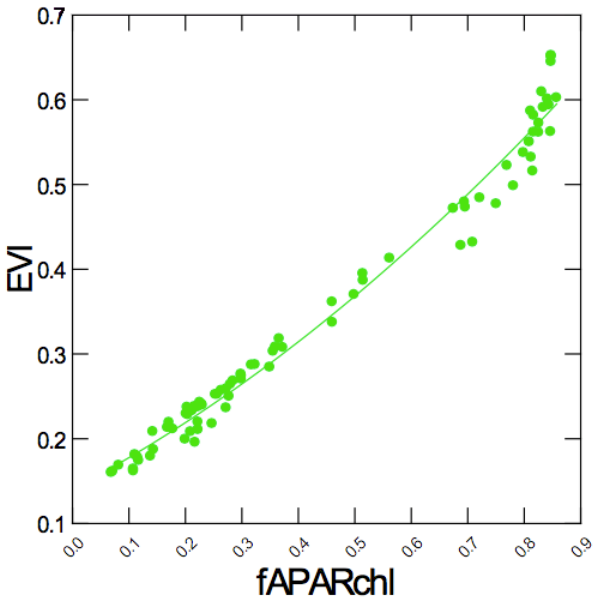

Vegetation Indices vs. APARchl

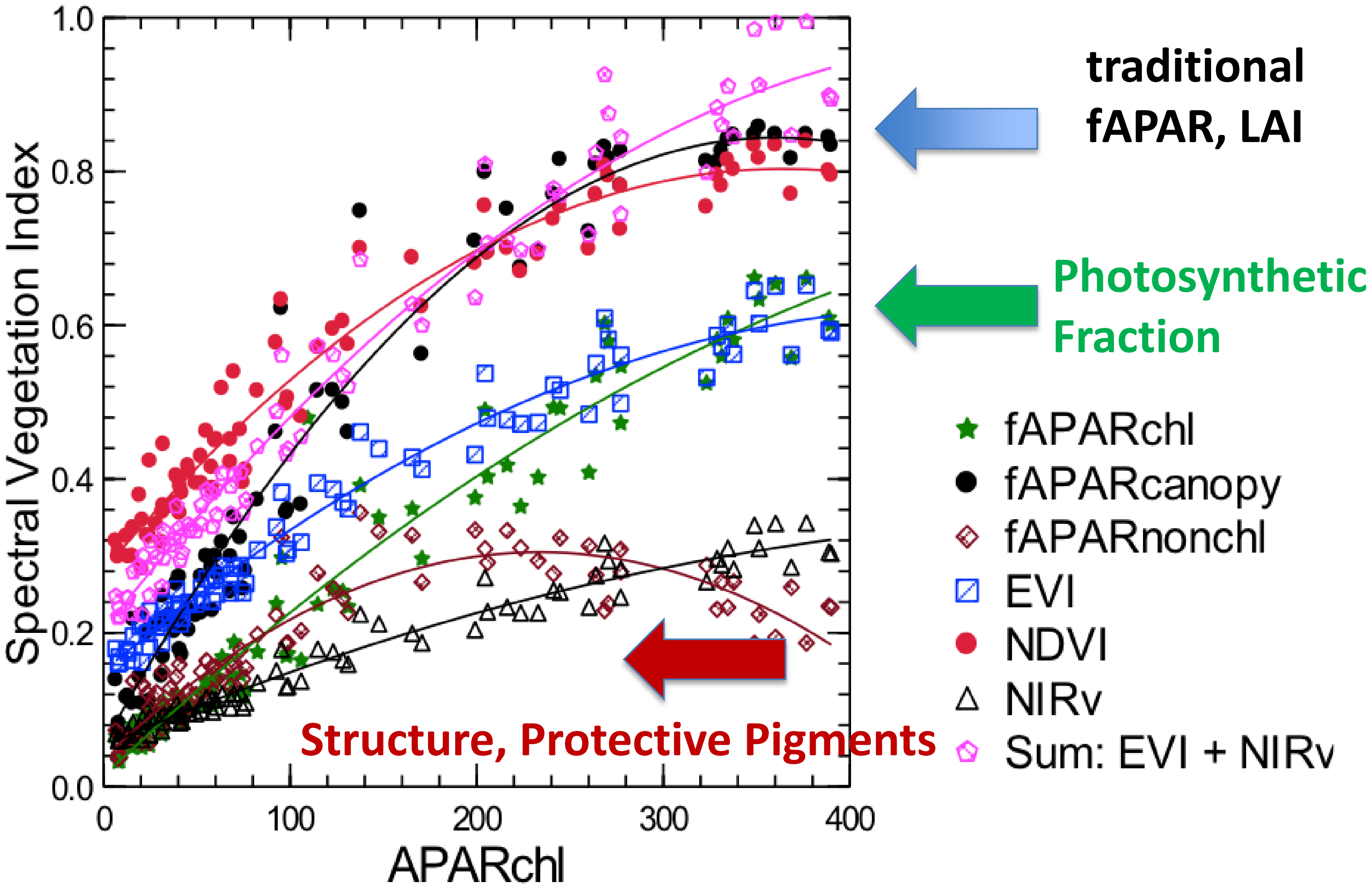

Far-Red SIF/cos(SZA) from GOME-2

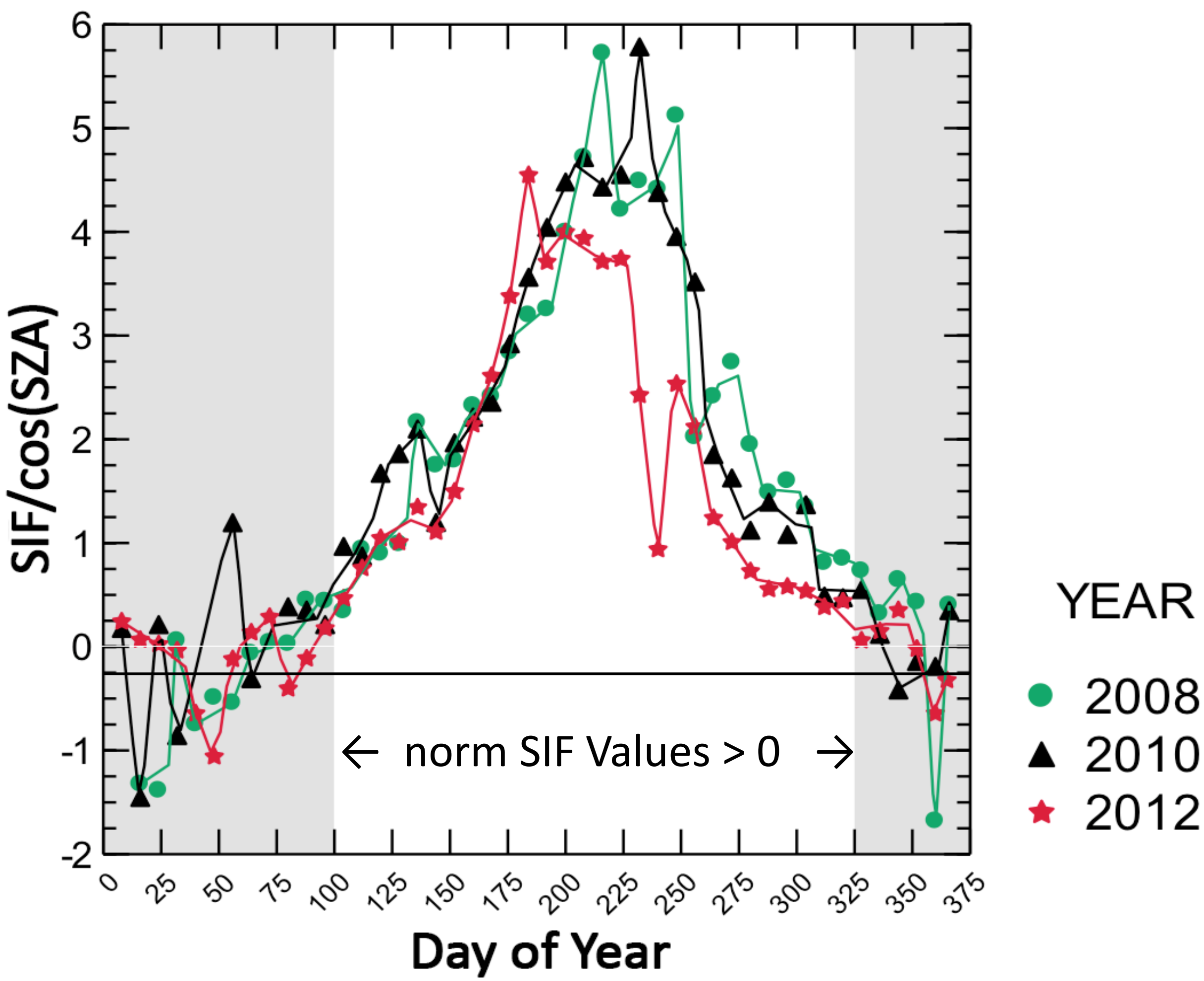

Annual patterns for 8-day averages of far-red SIF/cos(SZA) radiance (mW m^{-2} m^{-1} sr^{-1}) in 3 years retrieved from GOME-2, normalized with cos(SZA). Data represent 50 km x 50 km regions centered on the Nebraska research cornfield site (US-NE1).
The "green period" is defined as DOYs 100 - 325 (SIF > 0).

Far-Red SIF/cos(SZA) vs. APARchl in 2010

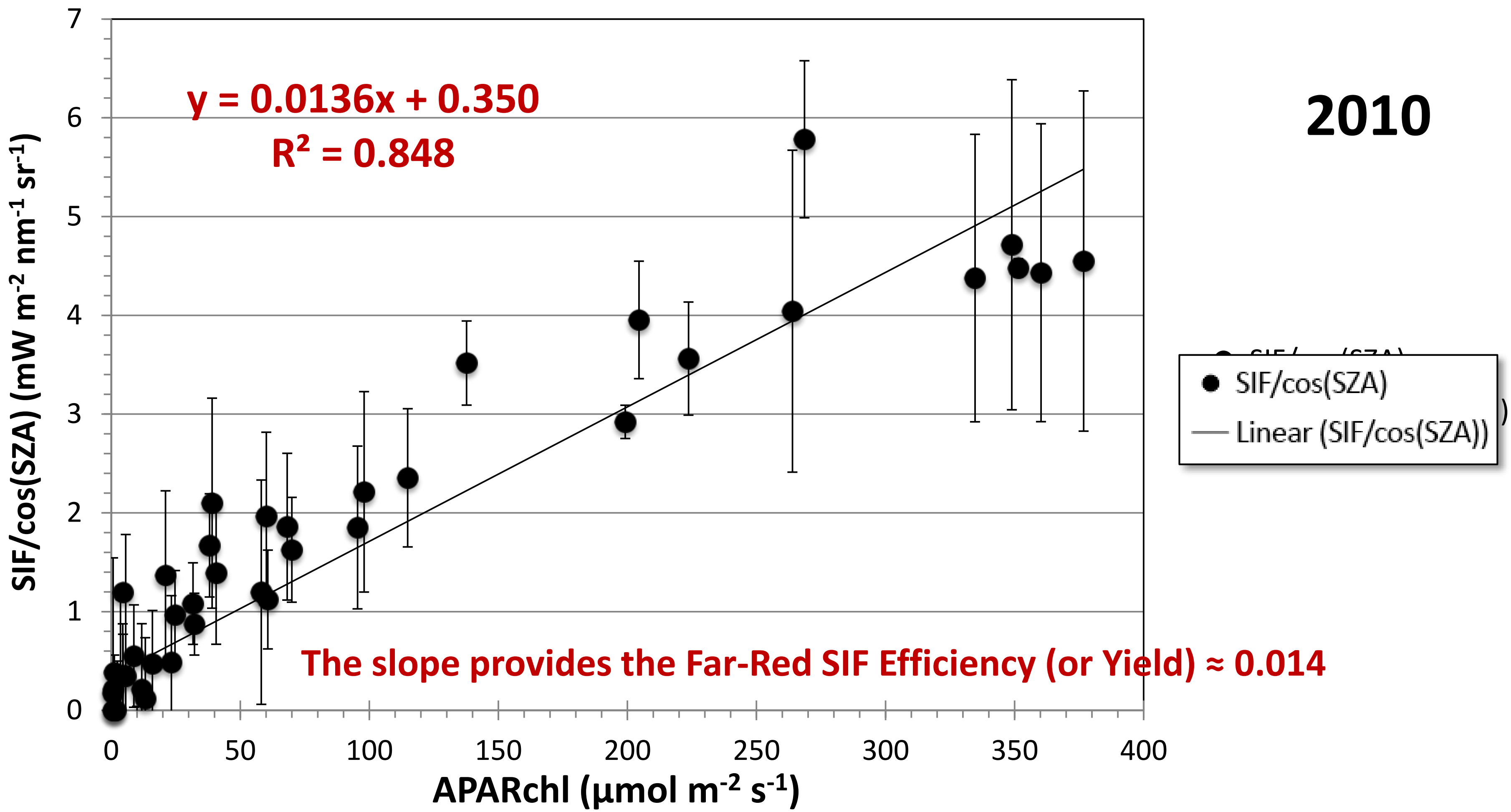

Full year 2010 linear relationship between normalized far-red SIF radiance (mW m^{-2} m^{-1} sr^{-1}) & APARchl (µmol m^{-2} s^{-1}). The SIF values are 8-day averages (± SD) GOME-2 retrievals.

<u>No negative SIF values were included</u>.

The fAPARchl values are derived from 8-day standard Terra MODIS products.

Far-Red SIF/cos(SZA) vs. fAPARchl in 2010

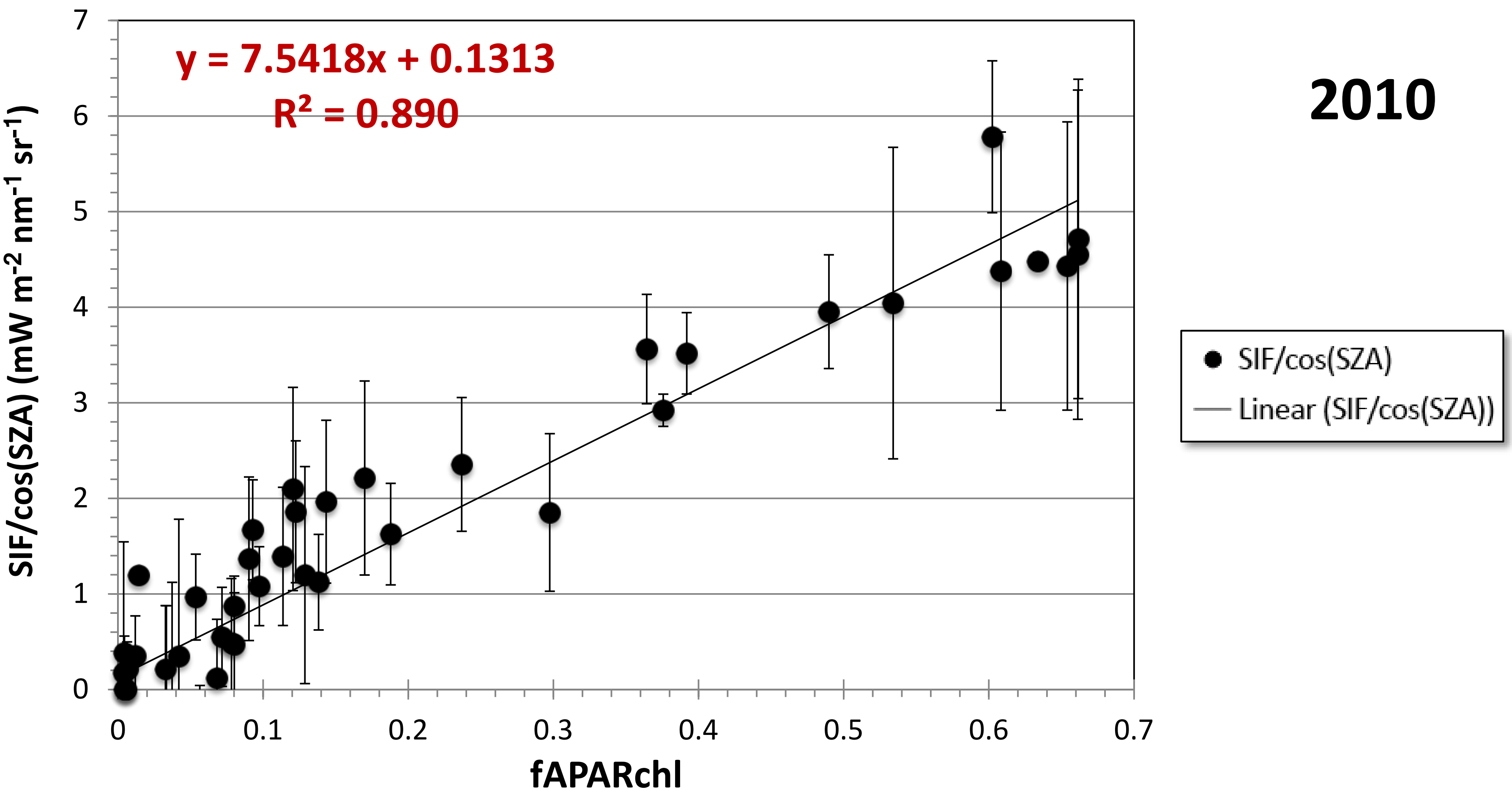

Full year 2010 linear relationship between SZA-normalized far-red SIF radiance ($mW\ m^{-2}\ m^{-1}\ sr^{-1}$) & fAPARchl. The SIF values are 8-day averages (± SD) GOME-2 retrievals.

<u>No negative SIF/cos(SZA) values were included</u>.

The fAPARchl values are derived from 8-day standard Terra MODIS products.

SIF Yields from SIF/cos(SZA) vs. APARchl

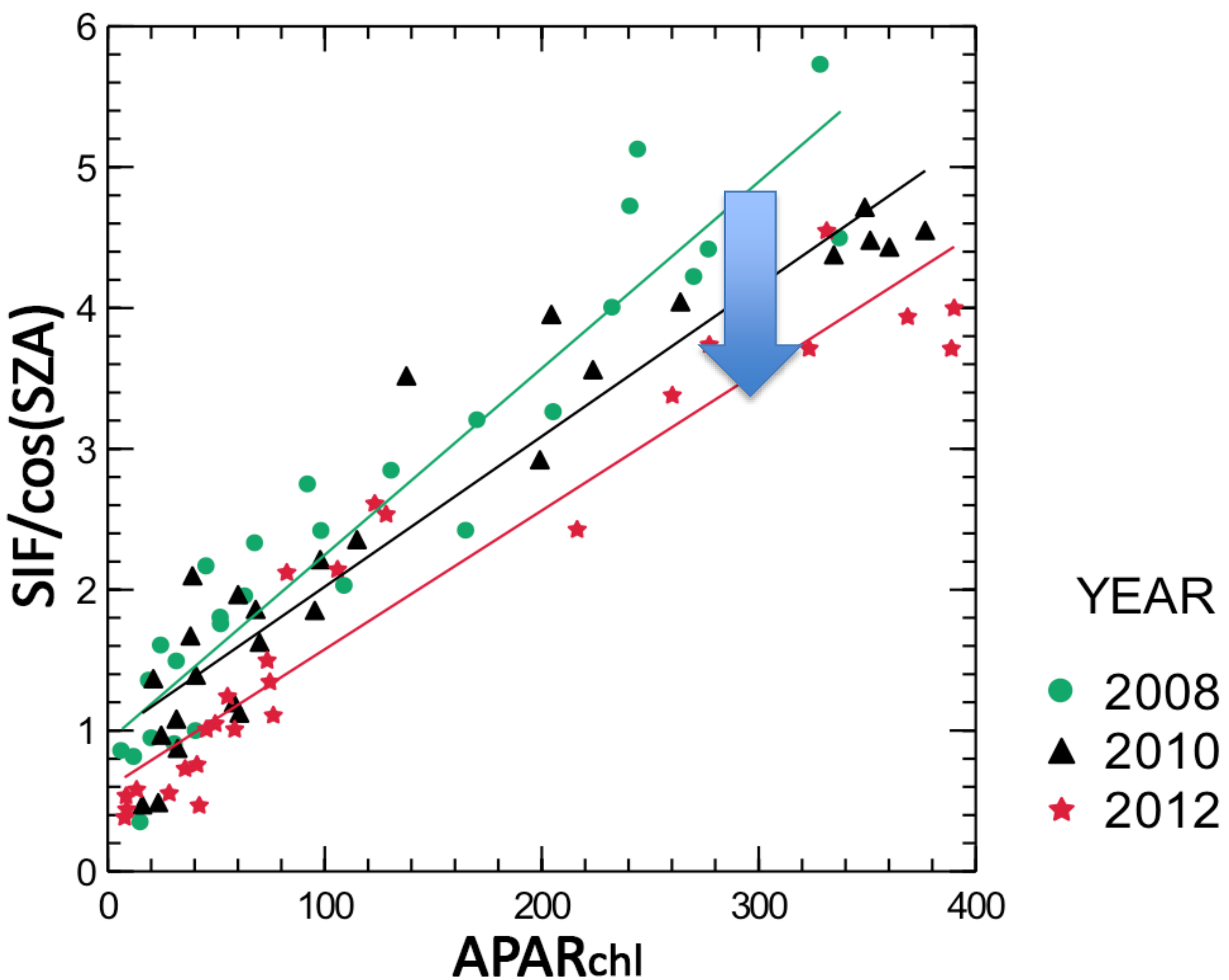

Linear relationships in 3 years: SIF/cos(SZA) (mW m^{-2} m^{-1} sr^{-1}) & APARchl (µmol m^{-2} s^{-1}), for the "green" season period (DOY 100 – 325).

The annual and regional SIFyields (J μmol^{-1} APAR sr^{-1} nm^{-1}) were estimated from the slopes: 1 % to 1.4% ($p \leq 0.01$): 2008 (0.0165); 2010 (0.0136); and 2012 (0.0115).

Vegetation Indices vs. SIF/cos(SZA)

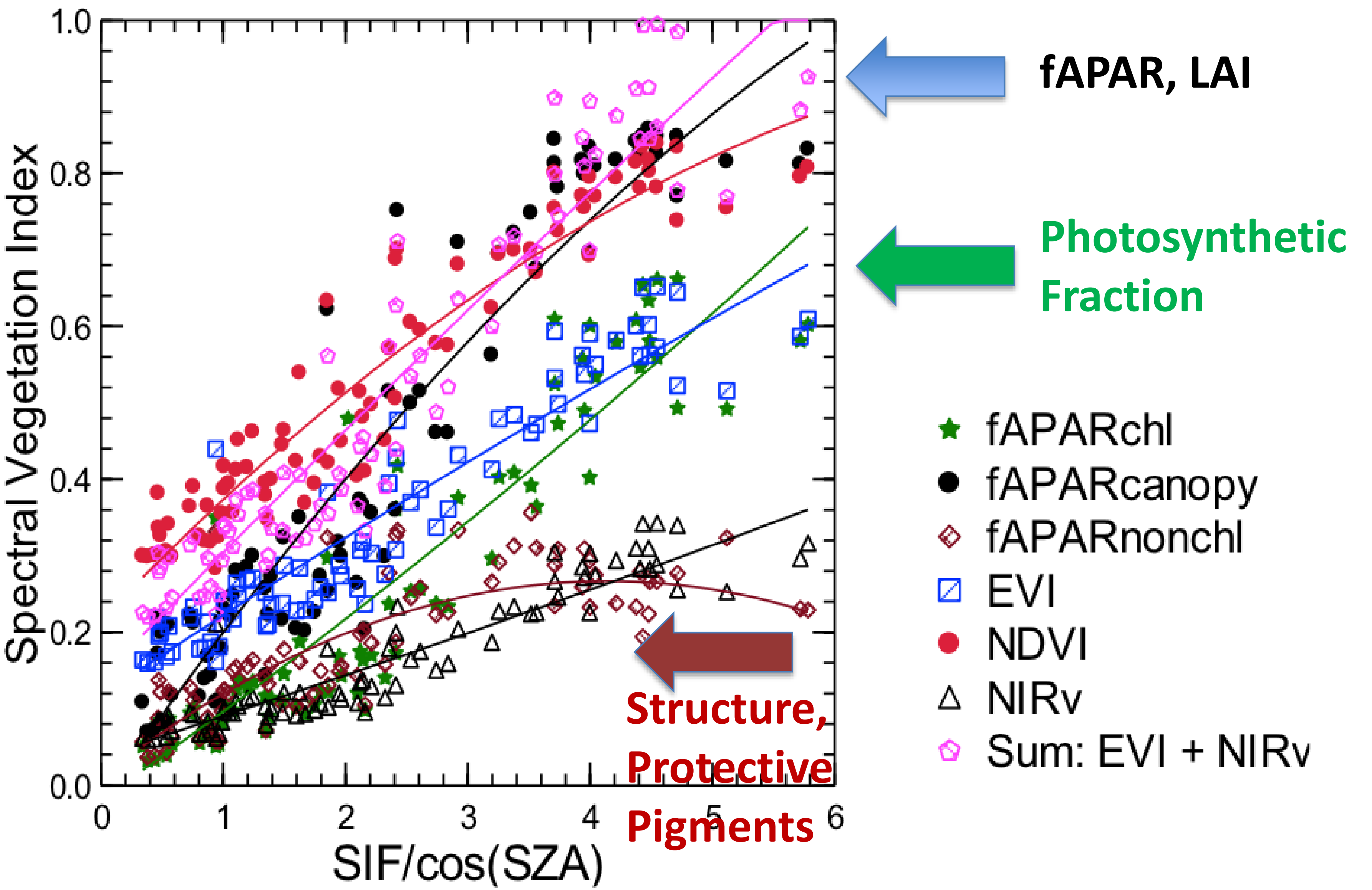

Seasonal SIF Yields 2008, 2010, 2012

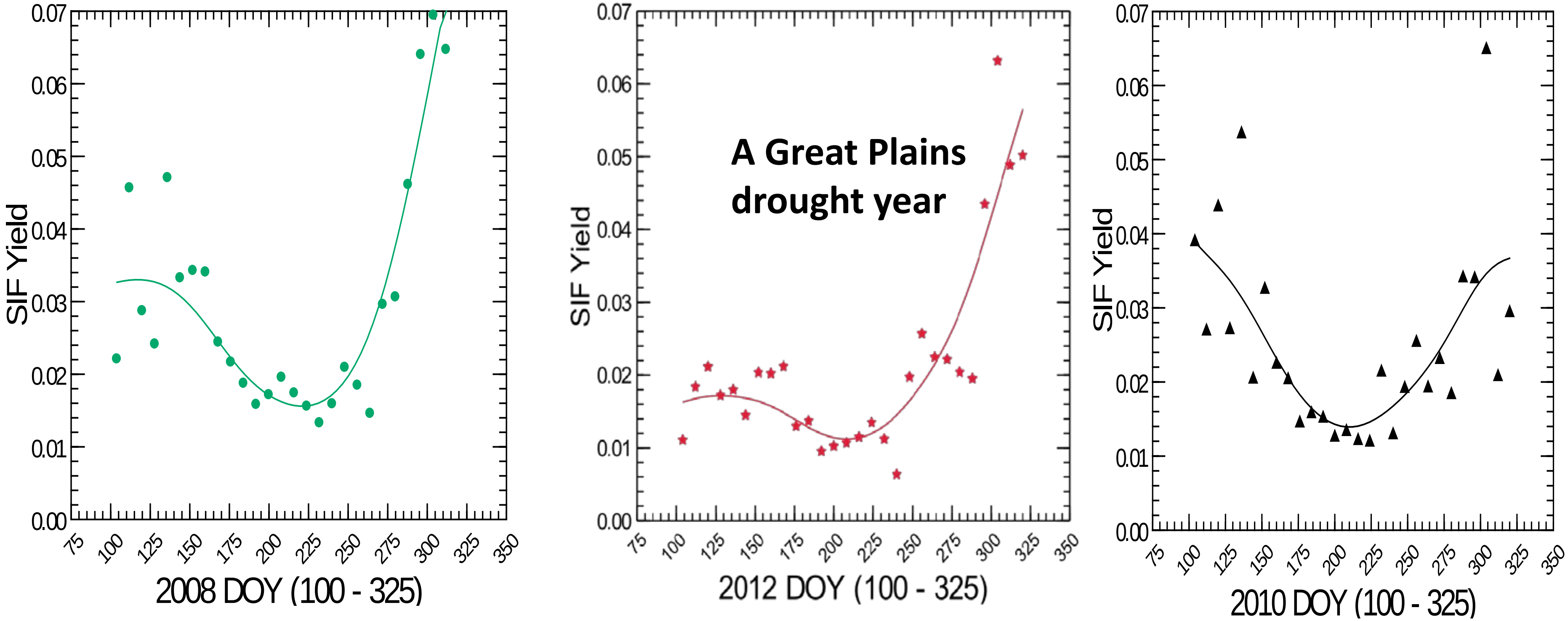

The SIF Yield (SIFϕ) varies throughout the "green" season (DOY 100-325). The SIFϕ was lowest (0.01 – 0.02) during the 70 mid-season days (DOY 175 – 245).

Far-Red SIF Yields

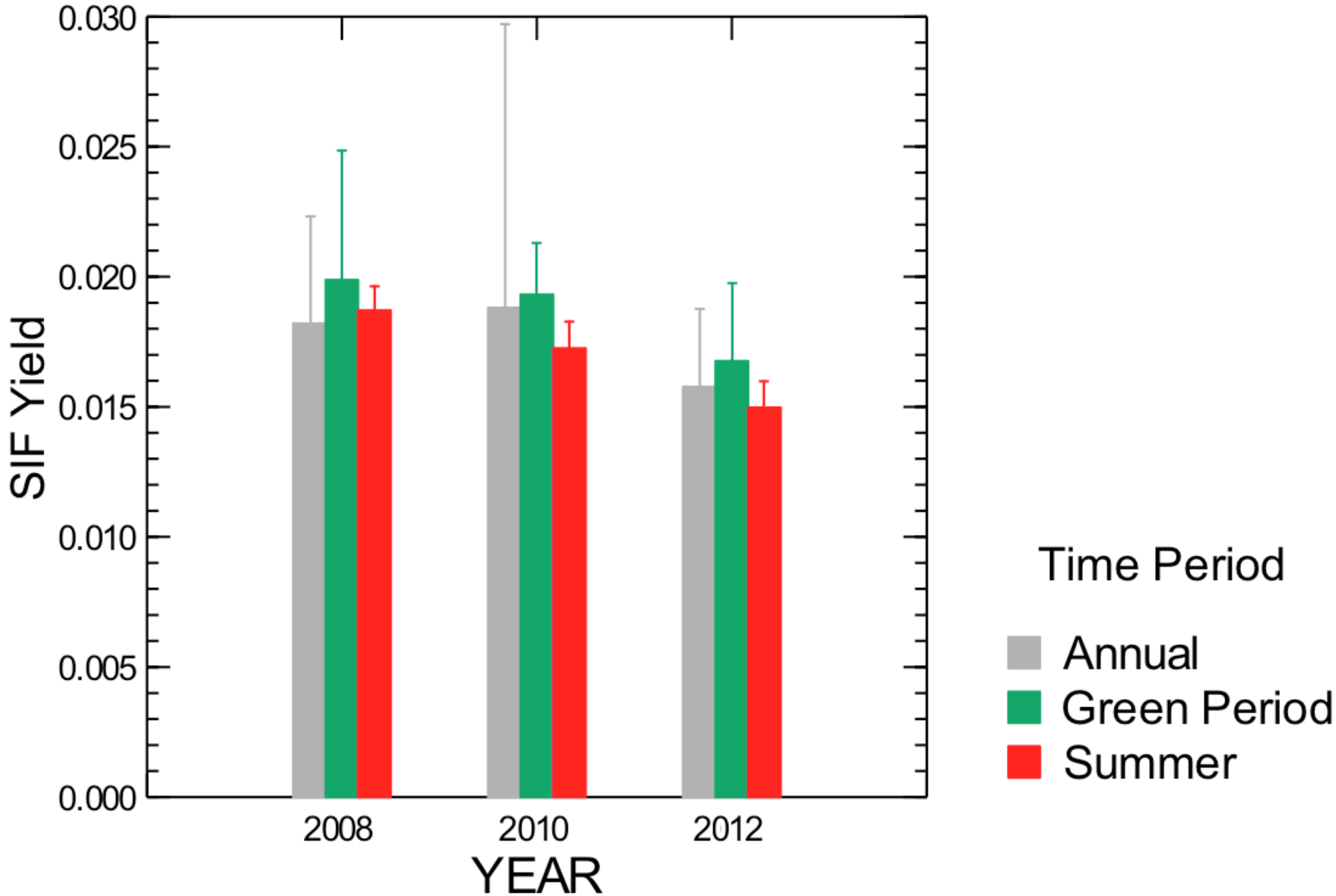

Comparison of the average far-red SIF Yields computed over three time periods per year: the full year, the green period (DOY 100 – 328), and the summertime (DOY 125 – 248). Negative values were excluded.

Conclusions

- We described *physically – based* canopy variables and their relationship to Far-Red SIF from orbital observations (GOME-2, MODIS).
- We found 3 groups of Canopy Spectral Veg. Variables:
  - * Chlorophyll-containing: fAPARchl and EVI
  - * Non-Chl containing: fAPARnonchl and NIRv
  - * Total Canopy (~ fPAR, LAI):

    fAPARcanopy Sum: EVI + NIRv NDVI
- We examined the seasonal behavior of the variables in 3 years for an agricultural region (aka the corn belt).
- We obtained annual & seasonal estimates of SIF yield.
- Spectral Variables are <u>non-linearly</u> related to APARchl.
- Spectral Variables are <u>linearly related</u> to SIF/cos(SZA).

FLEX mission concept

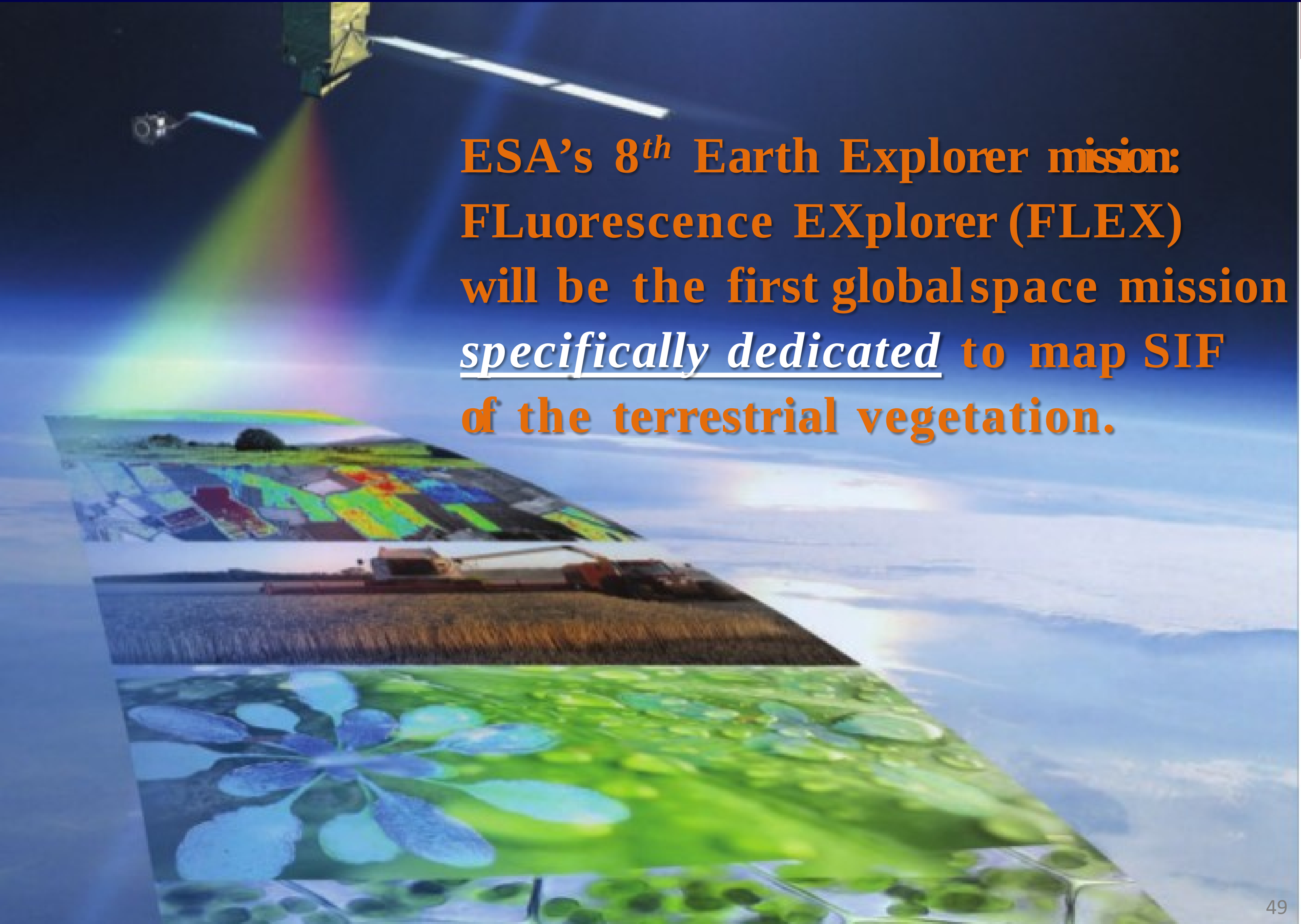

ESA's 8th Earth Explorer mission: FLuorescence EXplorer (FLEX) will be the first global space mission *specifically dedicated* to map SIF of the terrestrial vegetation.

NASA Corn Maze
Mars Rover
Cornbelly's
in Lehi, Utah

THANK YOU!

Special thanks to David Landis SGT, NASA/GSFC
For graphics

Bio-physical Parameters and GPP: USDA/Beltsville, MD Cornfield

Bio-physical parameters
(in order of importance)

Senescent material - Cs (a.u, 1&2)
Leaf dry mater - Cdm (g cm^{-2}, 3)
Leaf inclination - LIDF (4)
Leaf water content - Cw (g cm^{-2}, 5)
Leaf Area Index - LAI (6)
Leaf Chlorophyll - Cab (µg cm^{-2}, 7)
Leaf Carotenoids - Cca (µg cm^{-2}, 8)